



Nitrogen chemistry and speciation in low-temperature geothermal waters, Iceland

Ragnheiður Steinunn Ásgeirs dóttir



**Faculty of Earth Sciences
University of Iceland
2016**

Nitrogen chemistry and speciation in low-temperature geothermal waters, Iceland

Ragnheiður Steinunn Ásgeirsdóttir

60 ECTS thesis submitted in partial fulfillment of a
Magister Scientiarum degree in Geology

Advisor
Andri Stefánsson

Faculty of Earth Sciences
School of Engineering and Natural Sciences
University of Iceland
Reykjavik, January 2016

Nitrogen chemistry and speciation in low-temperature geothermal waters, Iceland
N chemistry of Icelandic low-T geothermal waters
60 ECTS thesis submitted in partial fulfillment of a *Magister Scientiarum* degree in
Geology

Copyright © 2016 Ragnheiður Steinunn Ásgeirsdóttir
All rights reserved

Faculty of Earth Sciences
School of Engineering and Natural Sciences
University of Iceland
Sturlugata 7
101, Reykjavík
Iceland

Telephone: 525 4000

Bibliographic information:
Ragnheiður Steinunn Ásgeirsdóttir, 2016, *Nitrogen chemistry and speciation in low-temperature geothermal waters, Iceland*, Master's thesis, Faculty of Earth Sciences, University of Iceland, pp. 59.

ISBN XX

Printing: Háskólaprent
Reykjavík, Iceland, febrúar 2016

Abstract

Nitrogen in geothermal systems occurs mostly as N₂, NH₄, NO₃, NO₂ and organic nitrogen. Based on isotope studies, geothermal fluids in Iceland are considered to be derived from meteoric water, seawater and/or magma. N₂ predominates in high-temperature waters whereas NH₄, NO₃, NO₂ have been observed in low-temperature geothermal waters. Limited data are, however, on all the nitrogen oxidation states in a given water, i.e. N₂, NH₄, NO₃, NO₂ and organic nitrogen, and the source of individual oxidation states has not been systematically studied. In this study, all the nitrogen species were determined in low-temperature waters in Iceland, and from those data the reactions and possible sources of various oxidation states were assessed. Altogether, 34 samples of springs, wells and streams were collected and major elemental and various nitrogen species concentrations determined, including N₂, NH₄, NO₂, NO₃ and organic nitrogen. The sampled waters had temperatures of 2-125°C, pH of 2.48-9.72 and total dissolved solids between 801 and 31645 µmol/L. Dissolved N₂ was the most abundant species with concentrations of 44-634 µmol/L and counting for up to 100% of nitrogen in the samples. Other nitrogen concentrations were ammonium, ranging from <0.1-95 µmol/L, nitrite and nitrate concentrations were <0.1-0.66 µmol/L and <0.1-8.51 µmol/L respectively and organic nitrogen concentrations varied from 0-9.44 µmol/L. Various reactions between the oxidation states were studied by calculations of redox potentials for given redox pairs. For all water types, a redox disequilibrium prevails between various nitrogen containing reactions. Possible nitrogen-redox reactions within the system may be summarized into four groups: (1) nitrogen fixation, (2) nitrification, (3) denitrification and (4) organic matter decomposition. Based on the reaction order and affinity calculations, several possible N-containing reactions were observed, including nitrogen fixation and nitrification. The source of N₂ may be considered to be atmospheric and denitrification, assuming limited deep mantle N₂ source. As observed, most waters are undersaturated with respect to atmospheric N₂, suggesting a possible reduction of N₂ to NH₄⁺. The source of NO₃ and NO₂ may also be the source water, i.e. it does not produce upon reactions within the system. The origin of N_{residual} is considered to be from dissolved organic matter.

Útdráttur

Köfnunarefni í jarðhitakerfum kemur oftast fyrir sem N₂, NH₄⁺, NO₃, NO₂ og lífrænt köfnunarefni. Samkvæmt rannsóknum á ísótópum eru jarðhitavökvar á Íslandi taldir vera upprunalega regnvatn, sjór og/eða kvika. Í háhitavatni er mest af N₂ en NH₄⁺, NO₃ og NO₂ hafa einnig verið mæld í lághitavatni. Þó er lítið til af gögnum um öll oxunarstig köfnunarefnis í gefnu vatni, þ.e. N₂, NH₄⁺, NO₃, NO₂ og lífrænt köfnunarefni, og uppruni hvers oxunarstigs hefur ekki verið rannsakaður markvisst. Í þessari rannsókn voru allar tegundir köfnunarefnis ákvárdar í lágitavatni á Íslandi, og út frá þessum upplýsingum voru hvörf og hugsanlegur uppruni mismunandi oxunarstiga metinn. Í heildina voru tekin 34 sýni af uppsprettum, borholum og lækjum og greind voru úr þeim aðalefni og mismunandi tegundir köfnunarefnis, þ.a.m. N₂, NH₄⁺, NO₃ og lífrænt N. Við söfnun höfðu sýnin hitastig á bilinu 2-125°C, pH 2.48-9.72 og heildarmagn uppleysts efnis var 801-31645 μmol/L. Upplést N₂ var algengasta tegundin með styrk upp á 44-634 μmol/L og taldist því til allt að 100% alls köfnunarefnis í sýnunum. Styrkur annara N tegunda voru ammoníum, <0.1-95 μmol/L, nítrít og nítrat voru <0.1-0.66 μmol/L og <0.1-8.51 μmol/L hvort um sig og styrkur lífræns köfnunarefnis var 0-9.44 μmol/L. Ýmis hvörf á milli oxunarstiga voru skoðuð með útreikningum á afoxunarmætti gefinna oxunarpara. Fyrir allar vatnsteigdir var oxunarójafnvægi milli efnahvarfa sem innihéldu köfnunarefni. Hugsanleg oxunarhvörf fyrir nitur í kerfinu má flokka í fjóra flokka: (1) niturnám, (2) nítratmyndun, (3) afnítrun og (4) niðurbrot lífræns efnis. Byggt á röð efnahvarfanna og virkni þeirra, voru hvörf skoðuð sem innihéldu köfnunarefni skoðuð, þ.a.m. niturnám og nítratmyndun. Uppruni N₂ er talinn vera andrúmsloft og afnítrun, þegar gert er ráð fyrir takmörkuðum uppruna frá móttli. Sést að flestar vatnsteigdir eru undirmettaðar með tilliti til N₂ úr andrúmslofti sem bendir til afoxunar á N₂ í NH₄⁺. Uppruni NO₃ og NO₂ er einnig mögulega uppruni vatnsins, þ.e. það myndast ekki með efnahvörfum innan kerfisins. Uppruni N_{residual} er talinn vera upplést lífrænt efni.

Table of Contents

List of Figures	viii
List of Tables.....	x
Acknowledgements	xi
1 Introduction.....	1
2 Sampling and analysis	3
2.1 Sampling and analysis	3
2.2 Geochemical modeling.....	5
3 Chemical composition of the water samples collected.....	13
3.1 Major elements	13
3.2 Nitrogen compounds	14
4 Discussion	19
4.1 Aqueous speciation of nitrogen compounds	19
4.2 Electron potential and half redox reactions	20
4.3 Overall redox reactions, reaction order and reaction energies	23
4.4 Source and reactions of N-containing compounds.....	28
4.5 Comparisons to other systems	32
5 Summary and conclusions.....	33
References.....	35
Appendix A.....	37
Appendix B	38
Appendix C.....	41
Appendix D.....	44
Appendix E.....	47

List of Figures

<i>Figure 1 Map of sampling locations in Iceland.</i>	3
<i>Figure 2 A typical setting for sampling spring water. Photo A) showing 1. A silicone tube leading to a cold stream, 2. A peristaltic pump, 3. A filter and 4. A sampling bottle or in this case, a bucket. Photo B) shows a typical setup of well sampling where tubing is fitted to 1. A well head leading to 2. A cooling coil submerged into cold water. From there a silicone tube leads to 3. A filter holder and from there to 4. A sample bottle. The setup is the same for hot springs, except the tubing leads to a hot spring instead of a well head.....</i>	4
<i>Figure 3 A) The relationship between in situ pH and temperature in all samples showing the differences between non-thermal waters (open circles), NaCl waters (black triangles) and acid-sulfate waters (open squares) and B) The relationship between temperature and total dissolved solids. The legends are the same as in A.</i>	13
<i>Figure 4 The distribution of A) $\sum CO_2$- SO_4-Cl and B) Ca+Mg- K-Na for natural waters in Iceland. These triangle plots are used to categorize the waters. Steam-heated acid-sulfate waters are distinctive in both plots. The legends are the same as in Figure 3.</i>	14
<i>Figure 5 The distribution of nitrogen species in geothermal waters in Iceland.</i>	14
<i>Figure 6 The distribution of A) N_2-NH_4-NO_2^-+NO_3^-+$N_{residual}$ and B) NH_4-NO_2^-+NO_3^--$N_{residual}$. Symbols have the same notations as Figure 4. These triangle plots, as well as the boxplot in Figure 5, are used to determine nitrogen species of importance. As can be seen in Figure A, the most important species is N_2.</i>	15
<i>Figure 7 Aqueous species distribution of nitrogen in geothermal waters in Iceland.</i>	19
<i>Figure 8 Calculated redox potentials for half reactions of interest.</i>	20
<i>Figure 9 Affinities for reactions #100 ($2H^+$ + $0.5O_{2(aq)}$ + $2e^-$ = H_2O half reaction as electron acceptor). The symbols in the figure represent the pH and temperature of each sample and their calculated affinities. The affinities are calculated from analytical data in Table 5 for the first set of reactions given in Table 4. The lines represent trends with each reaction given in Table 4.</i>	25
<i>Figure 10 Affinities for reactions #200 ($2H^+$ + $2e^-$ = $H_{2(aq)}$ half reaction as electron acceptor) plotted with temperature and pH.</i>	25

<i>Figure 11 Affinities for reactions #500 ($SO_4^{2-} + 10H^+ + 8e^- = H_2S_{(aq)} + 4H_2O$ half reaction as an electron acceptor) plotted with temperature and pH.</i>	25
<i>Figure 12 Affinities for reactions #2100 ($NO_3^- + 10H^+ + 8e^- = NH_4^+ + 3H_2O$ half reaction as electron acceptor) plotted with temperature and pH.</i>	26
<i>Figure 13 Affinities for reactions #2200 $NO_2^- + 8H^+ + 6e^- = NH_4^+ + 2H_2O$ half reaction as electron acceptor) plotted with temperature and pH.</i>	26
<i>Figure 14 Affinities for reactions #2300 ($N_2(aq) + 8H^+ + 6e^- = 2NH_4^+$ half reaction as electron acceptor) plotted with temperature and pH.</i>	26
<i>Figure 15 Affinities for reactions #2400 ($2NO_2^- + 8H^+ + 6e^- = N_2(aq) + 4H_2O$ half reaction as electron acceptor) plotted with temperature and pH.</i>	27
<i>Figure 16 Affinities for reactions #2500 ($2NO_3^- + 12H^+ + 10e^- = N_2(aq) + 6H_2O$ half reaction as electron acceptor) plotted with temperature and pH</i>	27
<i>Figure 17. Affinities for reactions #2600 ($NO_3^- + 2H^+ + 2e^- = NO_2^- + H_2O$ as electron acceptor) plotted with temperature and pH</i>	27
<i>Figure 18 A) Concentrations of $N_2(aq)$ versus temperature compared with saturation line of N_2 in the atmosphere, and B) The ratio of N_2/Ar versus temperature showing that the samples plot between the lines of N_2/Ar ratios in air (green line) and the saturation line of N_2/Ar (red line), supporting that the source for N_2 is atmospheric.</i>	29
<i>Figure 19 The relationship between marine Cl (mClm) and measured NO_3 and NO_2 concentration.</i>	30
<i>Figure 20 The relationship of N_{residual} with other nitrogen oxidation states and dissolved organic matter (DOC).</i>	31

List of Tables

<i>Table 1 Sampling and analytical methods</i>	5
<i>Table 2 The logarithm of the equilibrium constant (K) for selected reactions at 0-350°C and p_{sat}. The values are taken from the ChemEn database of the Geysir group, Univeristy of Iceland if not otherwise indicated</i>	7
<i>Table 3 The definition of pe values for reactions of interest. Values for logK are given in Table 2.</i>	8
<i>Table 4 The logarithm of the equilibrium constant (K) for selected redox reactions at 0-350°C and p_{sat}. The values are taken from the ChemEn database of the Geysir group, Univeristy of Iceland</i>	9
<i>Table 5 Chemical compostion of major elements, dissolved gases and nutrients in geothermal water, Iceland. Units are in $\mu\text{mol/L}$.</i>	16
<i>Table 6 Aqueous species activities</i>	22

Acknowledgements

Firstly I would like to thank my supervisor, Andri for helping me with this project and encouraging independent work. This will help me the most in the future. Hanna gets my best thanks for her assistance, from setting up the project to helping me writing the thesis and everything in between. Then I want to thank Nicole for great sampling trips as well as helping me with analysis. Eyðís I would like to thank for helping me with all nitrogen analysis and teaching me so much as well as various discussions in the smallest lab. Ríkey for fun times at long hours in Askja and keeping me somewhat positive.

My friends and coworkers at ÍSOR, especially Finnbogi, Heimir and Sylvía Rakel, thank you for all your help as well as all the fun times during the last few years.

Last, but definitely not the least, my family; mom, dad and Brynjar, both for helping me with the project as well as listening to me complaining.

This thesis was funded by the Landsvirkjun Research Fund (Orkurannsóknarsjóður) and was very much appreciated.

1 Introduction

Nitrogen in geothermal systems occurs in various oxidation states, as N₂ and NH₃ gas in the vapor phase and as dissolved ΣNH_4 , N₂, NO₃, NO₂ and organic N in the liquid phase. The nitrogen in geothermal fluids has been attributed to various sources including atmospheric, mantle and sedimentary (Clor et al., 2005; Fischer et al., 2009; Fischer et al., 2002; Goff and Janik, 2002; Hedlund et al., 2011; Holloway et al., 2011; Lowenstern et al., 2012; McCleskey et al., 2010; Sano et al., 1998; Sano et al., 2001).

Based on major elemental composition, $\delta^2\text{H}$ and $\delta^{18}\text{O}$ systematics, it has been concluded that geothermal fluids in Iceland originate from meteoric water or seawater, or a mixture of those, as well as some components of magmatic volatiles (Árnason, 1976, 1977; Arnórsson and Andrésdóttir, 1995). The source of nitrogen compounds and reactivity is however less understood. In geothermal waters in Iceland, N₂ is considered to originate dominantly from the atmosphere (Arnórsson, 1986) with other possible sources being decomposition of organic matter. This is evident from somewhat elevated N₂/Ar ratios relative to air-saturated water (Arnórsson, 1995). The average total inorganic nitrogen concentration in precipitation and non-thermal surface water in Iceland is ~9 µM and 4.4 µM, respectively (Gislason et al., 1996). In low-temperature waters (<150°C) at Skagafjörður, North-Iceland, ΣNH_4 , NO₃ and NO₂ concentrations are <0.005-0.48 µM, <0.001-232 µM and <0.1-6.9 µM, respectively, in waters with temperature of ~0-95°C and pH of ~6.2-10.5 (Stefánsson et al., 2005). In high-temperature waters (>150°C), N₂ and NH₃ are the dominant species with partial pressures in the reservoir fluids being 0.01-2.99 bar and 1.54-2.12·10⁻⁴ bar, respectively (Stefánsson and Arnórsson, 2002). Based on $\delta^{15}\text{N}$ isotope systematics of geothermal fluids it is evident that the source of N₂ in high-temperature fluids may be atmospheric and deep mantle degassing (Óskarsson et al., 2015; Valentino et al., 1999).

The speciation and reactions of nitrogen compounds in geothermal fluids may be influenced by cooling, boiling, steam condensation, temperature and microbial activity (Arnórsson et al., 2007; Fournier, 1989; Holloway et al., 2011). The redox reactions involving nitrogen may be kinetically slow and in disequilibrium (Stefánsson et al., 2005; Stumm and Morgan, 2012). The reaction progress from this disequilibrium to equilibrium conditions is the major energy source for chemosynthetic life in thermal ecosystems (Shock et al., 2010). The growth of these microorganisms is also often limited by lack of nutrients, trace elements, carbon compounds and water as well as too high or low temperatures (Heitz et al., 1996; Sand, 2003).

The object of this study was to determine the distribution and the main reactions among all the nitrogen species in low-temperature geothermal surface- and ground waters in Iceland. From these data, the source and reactions of nitrogen were assessed including quantification of inorganic energy available from those reactions and available for microorganisms.

2 Sampling and analysis

2.1 Sampling and analysis

Altogether, 34 water samples from springs, streams and wells were collected around Iceland in 2014. The sample locations are given in Figure 1. Further information about the sampling locations can be found in Appendix E. The sampling and analytical procedures have been described in details in Arnórsson et al. (2006) and are summarized in Table 1 and Figure 2.

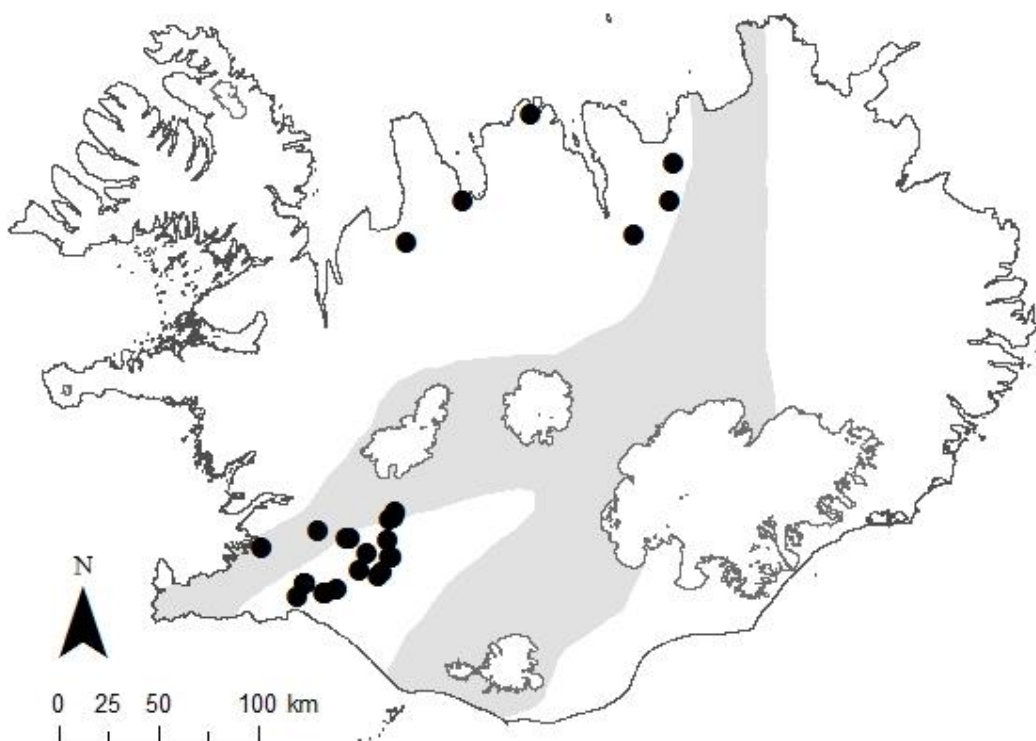


Figure 1 Map of sampling locations in Iceland.

Samples for determining major elements were filtered on-site through 0.2 μm cellulose acetate membrane and using a Teflon filter holder into 100 ml PP bottles (propylene). Samples for major cation determination (Si, B, Na, K, Ca, Mg, Fe, Al) were acidified using 1 ml HNO₃ (Suprapur®) to 100 ml samples followed by analysis by ICP-OES. Samples for determination of F and Cl were not further treated and analyzed using IC. In some cases the F concentration was analyzed using a F-selective electrode. For SO₄, analysis, 1 ml of 2M Zn-acetate solution was added to 100 ml filtered samples in order to precipitate H₂S. The ZnS particles were subsequently filtered off followed by IC analysis. Samples

for total dissolved inorganic carbon (ΣCO_2) and pH analysis were cooled down in-line and collected into amber glass bottles and analyzed using modified alkalinity titration and pH electrode, respectively. Dissolved H₂S was analyzed on site using Hg titration with dithiozone as an indicator.



Figure 2 A typical setting for sampling spring water. Photo A) showing 1. A silicone tube leading to a cold stream, 2. A peristaltic pump, 3. A filter and 4. A sampling bottle or in this case, a bucket. Photo B) shows a typical setup of well sampling where tubing is fitted to 1. A well head leading to 2. A cooling coil submerged into cold water. From there a silicone tube leads to 3. A filter holder and from there to 4. A sample bottle. The setup is the same for hot springs, except the tubing leads to a hot spring instead of a well head.

Samples for dissolved organic carbon (DOC) determination were filtered on-site through a 0.2 µm cellulose acetate membrane with a Teflon filter holder into acid washed 30 ml carbonate Nalgene bottles. The samples were acidified with 0.4 ml of 1.2 M HCl and stored at ~4°C until analyzed at Umeå Marine Research Institute.

Samples for nutrients analysis (NO₃, NO₂, $\sum\text{NH}_4$, N_{TOT}) were filtered on-site as previously described into acid washed 25 mL PP bottles. One sample bottle was collected for each nutrient analysis. The samples were cooled down in-line and on site and kept frozen until analyzed spectrophotometrically using a continuous flow autoanalyzer. Samples for N_{TOT} determination were oxidized using 0.2 ml 30% H₂O₂ in 10 ml sample followed by UV digestion for 4 hours and analyzed as NO₃⁻ spectrophotometrically on the autoanalyzer. Total oxidized nitrogen, the sum of nitrate and nitrite nitrogen and total residual N was taken to represent organic nitrogen; i.e.

$$\text{N}_{\text{residual}} = \text{N}_{\text{org}} = \text{N}_{\text{TOT}} - \text{NO}_3 - \text{NO}_2 - \sum\text{NH}_4.$$

Samples for determination of dissolved gases (H₂, N₂, O₂, Ar, CH₄) were collected into flow-through gas-tight bottles. The dissolved gases were extracted from the water samples in the laboratory using an ultrasonic bath followed by analysis using a GC.

Table 1 Sampling and analytical methods

Element	Sampling	Analytical method
Temperature	On-site	Thermometer
pH	Glass-bottle, untreated	Combination electrode
CO ₂	Glass-bottle, untreated	Modified alkalinity titration
H ₂ S	On-site	Hg-acetate titration
Si, B, Na, K, Ca, Mg, Fe, Al	Filtered (0.2µm), 1% HNO ₃	ICP-AES
F, Cl	Filtered (0.2µm)	IC
SO ₄	Zn-acetate, filtered (0.2µm)	IC
DOC	Carbonate nalgene, 0.4 mL HCl	
NH ₄	Filtered (0.2 µm)	Spectrophotometry
NO ₂ , NO ₃	Filtered (0.2 µm), frozen	Spectrophotometry
N _{TOT}	Filtered (0.2 µm), oxidized	Spectrophotometry
H ₂ , O ₂ , N ₂ , Ar, CH ₄	Gas-bulb	GC

2.2 Geochemical modeling

Geochemical calculations were carried out using the PHREEQC program and using the llnl.dat database (Parkhurst and Appelo, 1999) to gain insight into nitrogen processes and equilibrium speciation in geothermal waters in Iceland.

Three types of calculations were conducted: (1) aqueous speciation and mineral saturation was calculated for the sampled waters, (2) the electron potentials for half redox reactions were calculated for the sampled water from data on aqueous species activities and (3) the overall chemical energies were calculated for balanced redox reaction for the sampled water from data on aqueous species activities.

The calculations of aqueous speciation and mineral saturation for the sampled waters required a selection of temperature, here taken to be the temperature of sampling. The pH of the sampled waters was determined in the laboratory at ~20°C. These were converted to the pH of the measured waters, here referred as pH_T, assuming conservation of alkalinity (Arnórsson et al., 1982). Chemical reactions and their available chemical energies involving nitrogen compounds were assessed based on the electron potential (pe) and the chemical affinity of a reaction (A_r). The electron potential was defined for half chemical reactions according to,

$$pe = -\log a_e \equiv \log Q - \log K$$

where the a_e denotes the activity of the electron (e⁻) for a given redox half reaction and Q and K are the respective reaction quotients and equilibrium constants. The chemical affinity is defined for a balanced redox reaction according to,

$$A_r \equiv RT \ln(K/Q)$$

where R and T are the gas constant and absolute temperature. The equilibrium constant is linked to the Gibbs energy of reaction according to,

$$\Delta_r G^\circ = -RT \ln K$$

and the reaction quotient defined by,

$$Q = \prod_i (a_i)^{v_{i,r}}$$

where a_i represents the activity of the i^{th} compound in the reaction raised to its stoichiometric coefficient in the r -th reaction, $v_{i,r}$ which is positive for products and negative for reactants.

The redox reactions of interest and the definition of ρ_e are given in Tables 2 to 4. The equilibrium constants for the reactions were taken from the ChemEn database of the Geysir Research Group, University of Iceland (Stefánsson et al., in preparation).

Table 2 The logarithm of the equilibrium constant (K) for selected reactions at 0-350°C and p_{sat} . The values are taken from the ChemEn database of the Geysir group, University of Iceland if not otherwise indicated

# ^a	Reaction	e ⁻	logK _{25°C}	logK = a + bT + c/T + dlogT + fT ²			
				a	b	c	d
Oxygen half reaction							
1	H ₂ O = 2H ⁺ + 0.5O ₂ (aq) + 2e ⁻	2	-43,01	-253,7362	-0,115069	-6505,4646	106,11418
Hydrogen half reaction							
2	H ₂ (aq) = 2H ⁺ + 2e ⁻	2	3,11	313,1471	0,123789	-6651,5451	-129,35212
Sulfur half reactions							
5	H ₂ S(aq) + 4H ₂ O = SO ₄ ²⁻ + 10H ⁺ + 8e ⁻	8	-40,65	2104,6452	0,924221	-59724,1770	-882,89136
Nitrogen half reactions							
21	NH ₄ ⁺ + 3H ₂ O = NO ₃ ⁻ + 10H ⁺ + 8e ⁻	8	-119,13	894,7181	0,382532	-56043,8643	-373,88805
22	NH ₄ ⁺ + 2H ₂ O = NO ₂ ⁻ + 8H ⁺ + 6e ⁻	6	-91,36	915,4016	0,399278	-48545,7138	-382,95223
23	2NH ₄ ⁺ = N ₂ (aq) + 8H ⁺ + 6e ⁻	6	-31,03	-567,1148	-0,257100	6176,7958	235,30810
24	N ₂ (aq) + 4H ₂ O = 2NO ₂ ⁻ + 8H ⁺ + 6e ⁻	6	-151,69	2395,0217	1,054556	-103191,1663	-1000,02754
25	N ₂ (aq) + 6H ₂ O = 2NO ₃ ⁻ + 12H ⁺ + 10e ⁻	10	-207,23	2373,3624	1,028668	-118714,8494	-989,96937
26	NO ₂ ⁻ + H ₂ O = NO ₃ ⁻ + 2H ⁺ + 2e ⁻	2	-27,77	-19,4828	-0,016406	-7535,9090	8,59188
Gas solubilities							
	N ₂ (g) = N ₂ (aq) ^b		-3,19	-504,4237	-0,205868	13472,9811	206,0322
	O ₂ (g) = O ₂ (aq) ^b		-2,91	-555,3778	-0,2307395	14728,3018	227,6461

^aThe reaction number reference to the ChemEn database

^bCalculated using Supcrt92, slop08.dat database

Table 3 The definition of pe values for reactions of interest. Values for logK are given in Table 2.

Rxn #	Redox pair	Reaction	electron potential (pe)
Oxygen half reaction			
1	H ₂ O/O ₂	H ₂ O = 2H ⁺ + 0.5O ₂ (aq) + 2e ⁻	pe(H ₂ O/O ₂) = 1/2(0.5logaO ₂ (aq) + 2logaH ⁺ - logK)
Hydrogen half reaction			
2	H ₂ /H ⁺	H ₂ (aq) = 2H ⁺ + 2e ⁻	pe(H ₂ /H ⁺) = 1/2(2logaH ⁺ - logaH ₂ (aq) - logK)
Sulfur half reactions			
5	H ₂ S/SO ₄ ⁻²	H ₂ S(aq) + 4H ₂ O = SO ₄ ²⁻ + 10H ⁺ + 8e ⁻	pe(H ₂ S/SO ₄) = 1/8(logaSO ₄ ⁻² + 10logaH ⁺ - logaH ₂ S(aq) - logK)
Nitrogen half reactions			
21	NH ₄ ⁺ /NO ₃ ⁻	NH ₄ ⁺ + 3H ₂ O = NO ₃ ⁻ + 10H ⁺ + 8e ⁻	pe(NH ₄ /NO ₃) = 1/8(logaNO ₃ ⁻ + 10logaH ⁺ - logaNH ₄ ⁺ - logK)
22	NH ₄ ⁺ /NO ₂ ⁻	NH ₄ ⁺ + 2H ₂ O = NO ₂ ⁻ + 8H ⁺ + 6e ⁻	pe(NH ₄ /NO ₂) = 1/6(logaNO ₂ ⁻ + 8logaH ⁺ - logaNH ₄ ⁺ - logK)
23	NH ₄ ⁺ /N ₂	2NH ₄ ⁺ = N ₂ (aq) + 8H ⁺ + 6e ⁻	pe(NH ₄ /N ₂) = 1/6(logaN ₂ (aq) + 8logaH ⁺ - 2logaNH ₄ ⁺ - logK)
24	N ₂ /NO ₂ ⁻	N ₂ (aq) + 4H ₂ O = 2NO ₂ ⁻ + 8H ⁺ + 6e ⁻	pe(N ₂ /NO ₂) = 1/6(2logaNO ₂ ⁻ + 8logaH ⁺ - logaN ₂ (aq) - logK)
25	N ₂ /NO ₃ ⁻	N ₂ (aq) + 6H ₂ O = 2NO ₃ ⁻ + 12H ⁺ + 10e ⁻	pe(N ₂ /NO ₃) = 1/10(2logaNO ₃ ⁻ + 12logaH ⁺ - logaN ₂ (aq) - logK)
26	NO ₂ ⁻ /NO ₃ ⁻	NO ₂ ⁻ + H ₂ O = NO ₃ ⁻ + 2H ⁺ + 2e ⁻	pe(NO ₂ /NO ₃) = 1/2(logaNO ₃ ⁻ + 2logaH ⁺ - logaNO ₂ ⁻ - logK)

Table 4 The logarithm of the equilibrium constant (K) for selected redox reactions at 0-350°C and p_{sat} . The values are taken from the ChemEn database of the Geysir group, University of Iceland

#	Reaction	Donor	Acceptor	Rxn sum	e^-	$\log K = a + bT + c/T + d\log T + fT^2$				
$2H^+ + 0.5O_{2(aq)} + 2e^- = H_2O$ half reaction as electron acceptor										
100-1	$H_2(\text{aq}) + 0.5O_2(\text{aq}) = H_2O$	H_2 to H^+	O_2 to H_2O	[2]-[1]	2	566,8833	0,2389	-146,0805	-235,4663	-0,0001
100-20	$NH_4^+ + 2O_2(\text{aq}) = NO_3^- + 2H^+ + H_2O$	NH_4 to NO_3	O_2 to H_2O	[21]-4-[1]	8	1909,6629	0,8428	-30022,0057	-798,3448	-0,0004
100-21	$NH_4^+ + 1.5O_2(\text{aq}) = NO_2^- + 2H^+ + H_2O$	NH_4 to NO_2	O_2 to H_2O	[22]-3-[1]	6	1676,6102	0,7445	-29029,3199	-701,2948	-0,0003
100-22	$2NH_4^+ + 1.5O_2(\text{aq}) = N_2(\text{aq}) + 2H^+ + 3H_2O$	NH_4 to N_2	O_2 to H_2O	[23]-3-[1]	6	194,0938	0,0881	25693,1897	-83,0345	0,0000
100-23	$N_2(\text{aq}) + H_2O + 1.5O_2(\text{aq}) = 2NO_2^- + 2H^+$	N_2 to NO_2	O_2 to H_2O	[24]-3-[1]	6	3156,2302	1,3998	-83674,7724	-1318,3701	-0,0006
100-24	$N_2(\text{aq}) + H_2O + 2.5O_2(\text{aq}) = 2NO_3^- + 2H^+$	N_2 to NO_3	O_2 to H_2O	[25]-3-[1]	10	3642,0433	1,6040	-86187,5263	-1520,5403	-0,0007
100-25	$NO_2^- + 0.5O_2(\text{aq}) = NO_3^-$	NO_2 to NO_3	O_2 to H_2O	[26]-[1]	2	234,2534	0,0987	-1030,4444	-97,5223	0,0000
$2H^+ + 2e^- = H_{2(aq)}$ half reaction as electron acceptor										
200-1	$H_2O = 0.5O_2(\text{aq}) + H_2(\text{aq})$	H_2O to O_2	H^+ to H_2	[1]-[2]	2	-566,8833	-0,2389	146,0805	235,4663	0,0001
200-20	$NH_4^+ + 3H_2O = NO_3^- + 2H^+ + 4H_2(\text{aq})$	NH_4 to NO_3	H^+ to H_2	[21]-4-[2]	8	-357,8704	-0,1126	-29437,6837	143,5204	0,0000
200-21	$NH_4^+ + 2H_2O = NO_2^- + 2H^+ + 3H_2(\text{aq})$	NH_4 to NO_2	H^+ to H_2	[22]-3-[2]	6	-24,0398	0,0279	-28591,0784	5,1041	0,0000
200-22	$2NH_4^+ = N_2(\text{aq}) + 2H^+ + 3H_2(\text{aq})$	NH_4 to N_2	H^+ to H_2	[23]-3-[2]	6	-1506,5562	-0,6285	26131,4313	623,3644	0,0003
200-23	$N_2(\text{aq}) + 4H_2O = 2NO_2^- + 2H^+ + 3H_2(\text{aq})$	N_2 to NO_2	H^+ to H_2	[24]-3-[2]	6	1455,5803	0,6832	-83236,5309	-611,9712	-0,0003
200-24	$N_2(\text{aq}) + 6H_2O = 2NO_3^- + 2H^+ + 5H_2(\text{aq})$	N_2 to NO_3	H^+ to H_2	[25]-5-[2]	10	807,6267	0,4097	-85457,1237	-343,2088	-0,0002
200-25	$NO_2^- + H_2O = NO_3^- + H_2(\text{aq})$	NO_2 to NO_3	H^+ to H_2	[26]-[2]	2	-332,6299	-0,1402	-884,3639	137,9440	0,0001
$SO_4^{2-} + 10H^+ + 8e^- = H_2S_{(aq)} + 4H_2O$ half reaction as an electron acceptor										
500-1	$SO_4^{2-} + 2H^+ = H_2S + 2O_2(\text{aq})$	H_2O to O_2	SO_4 to H_2S	4[1]-[5]	8	-3119,5900	-1,3845	33702,3185	1307,3481	0,0006
500-2	$SO_4^{2-} + 4H_2(\text{aq}) + 2H^+ = H_2S(\text{aq}) + 4H_2O$	H_2 to H^+	SO_4 to H_2S	4[2]-[5]	8	-852,0567	-0,4291	33117,9965	365,4829	0,0002
500-20	$NH_4^+ + SO_4^{2-} = NO_3^- + H_2S(\text{aq}) + H_2O$	NH_4 to NO_3	SO_4 to H_2S	[21]-[5]	5	-1209,9271	-0,5417	3680,3128	509,0033	0,0002
500-21	$4NH_4^+ + 3SO_4^{2-} = 4NO_2^- + 2H^+ + 4H_2O + 3H_2S(\text{aq})$	NH_4 to NO_2	SO_4 to H_2S	4[22]-3-[5]	24	-2652,3292	-1,1756	-15010,3243	1116,8652	0,0005
500-22	$8NH_4^+ + 3SO_4^{2-} = 4N_2(\text{aq}) + 2H^+ + 12H_2O + 3H_2S(\text{aq})$	NH_4 to N_2	SO_4 to H_2S	4[23]-3-[5]	24	-8582,3950	-3,8011	203879,7145	3589,9065	0,0017
500-23	$4N_2(\text{aq}) + 3SO_4^{2-} + 4H_2O = 8NO_2^- + 2H^+ + 3H_2S(\text{aq})$	N_2 to NO_2	SO_4 to H_2S	4[24]-3-[5]	24	3266,1510	1,4456	-233592,1343	-1351,4361	-0,0006
500-24	$4N_2(\text{aq}) + 4H_2O + 5SO_4^{2-} = 8NO_3^- + 5H_2S(\text{aq})$	N_2 to NO_3	SO_4 to H_2S	4[25]-5-[5]	40	-1029,7767	-0,5064	-176238,5125	454,5793	0,0002
500-25	$4NO_2^- + SO_4^{2-} + 2H^+ = 4NO_3^- + H_2S(\text{aq})$	NO_2 to NO_3	SO_4 to H_2S	4[26]-[5]	8	-2182,5764	-0,9898	29580,5411	917,2589	0,0004

Table 4 continued

#	Reaction	Donor	Acceptor	Rxn sum	e ⁻		logK = a + bT + c/T + dlogT + fT ²	
<i>NO₃⁻ + 10H⁺ + 8e⁻ = NH₄⁺ + 3H₂O half reaction as electron acceptor</i>								
2100-1	H ₂ O + NO ₃ ⁻ + 2H ⁺ = 2O ₂ (aq) + NH ₄ ⁺	H ₂ O to O ₂	NO ₃ ⁻ to NH ₄ ⁺	4[1]-[21]	8	-1909,663	-0,843	30022,0 798,34 3,5894,E-04
2100-2	4H ₂ (aq) + NO ₃ ⁻ + 2H ⁺ = NH ₄ ⁺ + 3H ₂ O	H ₂ to H ⁺	NO ₃ ⁻ to NH ₄ ⁺	4[2]-[21]	8	357,870	0,113	29437,7 -143,52 -3,9222,E-05
2100-5	H ₂ S(aq) + H ₂ O + NO ₃ ⁻ = SO ₄ ²⁻ + NH ₄ ⁺	H ₂ S to SO ₄	NO ₃ ⁻ to NH ₄ ⁺	[5]-[21]	8	1209,927	0,542	-3680,3 -509,00 -2,3746,E-04
2100-21	NH ₄ ⁺ + 3NO ₃ ⁻ = 4NO ₂ ⁻ + 2H ⁺ + H ₂ O	NH ₄ to NO ₂	NO ₃ ⁻ to NH ₄ ⁺	4[22]-3[21]	24	977,452	0,450	-26051,3 -410,14 -1,9446,E-04
2100-22	5NH ₄ ⁺ + 3NO ₃ ⁻ = 4N ₂ (aq) + 2H ⁺ + 9H ₂ O	NH ₄ to N ₂	NO ₃ ⁻ to NH ₄ ⁺	4[23]-3[21]	24	-4952,614	-2,176	192838,8 2062,90 9,3771,E-04
2100-23	7H ₂ O + 4N ₂ (aq) + 3NO ₃ ⁻ = 8NO ₂ ⁻ + 2H ⁺ + 3NH ₄ ⁺	N ₂ to NO ₂	NO ₃ ⁻ to NH ₄ ⁺	4[24]-3[21]	24	6895,932	3,071	-244633,1 -2878,45 -1,3251,E-03
2100-24	4N ₂ (aq) + 9H ₂ O + 2H ⁺ = 3NO ₃ ⁻ + 5NH ₄ ⁺	N ₂ to NO ₃	NO ₃ ⁻ to NH ₄ ⁺	4[25]-5[21]	40	5019,859	2,202	-194640,1 -2090,44 -9,4699,E-04
2100-25	4NO ₂ ⁻ + H ₂ O + 2H ⁺ = 3NO ₃ ⁻ + NH ₄ ⁺	NO ₂ to NO ₃	NO ₃ ⁻ to NH ₄ ⁺	4[26]-[21]	8	-972,649	-0,448	25900,2 408,26 1,9412,E-04
<i>NO₂⁻ + 8H⁺ + 6e⁻ = NH₄⁺ + 2H₂O half reaction as electron acceptor</i>								
2200-1	H ₂ O + NO ₂ ⁻ + 2H ⁺ = 1.5O ₂ (aq) + NH ₄ ⁺	H ₂ O to O ₂	NO ₂ ⁻ to NH ₄ ⁺	3[1]-[22]	6	-1676,610	-0,744	29029,3 701,29 3,1782,E-04
2200-3	3H ₂ (aq) + NO ₂ ⁻ + 2H ⁺ = NH ₄ ⁺ + 2H ₂ O	H ₂ to H ⁺	NO ₂ ⁻ to NH ₄ ⁺	3[2]-[22]	6	24,040	-0,028	28591,1 -5,10 1,9197,E-05
2200-5	3H ₂ S(aq) + 4H ₂ O + 4NO ₂ ⁻ + 2H ⁺ = 3SO ₄ ²⁻ + 4NH ₄ ⁺	H ₂ S to SO ₄	NO ₂ ⁻ to NH ₄ ⁺	3[5]-4[22]	24	2652,329	1,176	15010,3 -1116,87 -5,1792,E-04
2200-21	H ₂ O + 4NO ₂ ⁻ + 2H ⁺ = 3NO ₃ ⁻ + NH ₄ ⁺	NH ₄ to NO ₃	NO ₂ ⁻ to NH ₄ ⁺	3[21]-4[22]	24	-977,452	-0,450	26051,3 410,14 1,9446,E-04
2200-22	NH ₄ ⁺ + NO ₂ ⁻ = N ₂ (aq) + 2H ₂ O	NH ₄ to N ₂	NO ₂ ⁻ to NH ₄ ⁺	[23]-[22]	6	-1482,516	-0,656	54722,5 618,26 2,8304,E-04
2200-23	N ₂ (aq) + 2H ₂ O = NO ₂ ⁻ + NH ₄ ⁺	N ₂ to NO ₂	NO ₂ ⁻ to NH ₄ ⁺	[24]-[22]	6	1479,620	0,655	-54645,5 -617,08 -2,8266,E-04
2200-24	3N ₂ (aq) + 8H ₂ O + 4H ⁺ + 5NO ₂ ⁻ = 6NO ₃ ⁻ + 5NH ₄ ⁺	N ₂ to NO ₃	NO ₂ ⁻ to NH ₄ ⁺	3[25]-5[22]	30	2543,079	1,090	-113416,0 -1055,15 -4,6717,E-04
2200-25	4NO ₂ ⁻ + H ₂ O + 2H ⁺ = 3NO ₃ ⁻ + NH ₄ ⁺	NO ₂ to NO ₃	NO ₂ ⁻ to NH ₄ ⁺	3[26]-[22]	6	-973,850	-0,448	25938,0 408,73 1,9421,E-04
<i>N₂(aq) + 8H⁺ + 6e⁻ = 2NH₄⁺ half reaction as electron acceptor</i>								
2300-1	3H ₂ O + N ₂ (aq) + 2H ⁺ = 1.5O ₂ (aq) + 2NH ₄ ⁺	H ₂ O to O ₂	N ₂ (aq) to NH ₄ ⁺	3[1]-[23]	6	-194,094	-0,088	-25693,2 83,03 3,4774,E-05
2300-2	3H ₂ + N ₂ (aq) + 2H ⁺ = 2NH ₄ ⁺	H ₂ to H ⁺	N ₂ (aq) to NH ₄ ⁺	3[2]-[23]	6	1506,556	0,628	-26131,4 -623,36 -2,6384,E-04
2300-5	3H ₂ S(aq) + 12H ₂ O + 4N ₂ (aq) + 2H ⁺ = 3SO ₄ ²⁻ + 8NH ₄ ⁺	H ₂ S to SO ₄	N ₂ (aq) to NH ₄ ⁺	3[5]-4[23]	24	8582,395	3,801	-203879,7 -3589,91 -1,6501,E-03
2300-21	9H ₂ O + 4N ₂ (aq) + 2H ⁺ = 3NO ₃ ⁻ + 5NH ₄ ⁺	NH ₄ to NO ₃	N ₂ (aq) to NH ₄ ⁺	3[21]-4[23]	24	4952,614	2,176	-192838,8 -2062,90 -9,3771,E-04
2300-22	2H ₂ O + N ₂ (aq) = NO ₂ ⁻ + NH ₄ ⁺	NH ₄ to NO ₂	N ₂ (aq) to NH ₄ ⁺	[22]-[23]	6	1482,516	0,656	-54722,5 -618,26 -2,8304,E-04
2300-23	2N ₂ (aq) + 4H ₂ O = 2NO ₂ ⁻ + 2NH ₄ ⁺	N ₂ to NO ₂	N ₂ (aq) to NH ₄ ⁺	[24]-[23]	6	2962,136	1,312	-109368,0 -1235,34 -5,6570,E-04
2300-24	8N ₂ (aq) + 18H ₂ O + 4H ⁺ = 6NO ₃ ⁻ + 10NH ₄ ⁺	N ₂ to NO ₃	N ₂ (aq) to NH ₄ ⁺	3[25]-5[23]	30	9955,661	4,372	-387028,5 -4146,45 -1,8824,E-03
2300-25	3NO ₂ ⁻ + 3H ₂ O + N ₂ (aq) + 2H ⁺ = 3NO ₃ ⁻ + 2NH ₄ ⁺	NO ₂ to NO ₃	N ₂ (aq) to NH ₄ ⁺	3[26]-[23]	6	508,666	0,208	-28784,5 -209,53 -8,8834,E-05

Table 4 continued

#	Reaction	Donor	Acceptor	Rxn sum	e ⁻		logK = a + bT + c/T + dlogT + fT ²			
$2NO_2^- + 8H^+ + 6e^- = N_{2(aq)} + 4H_2O$ half reaction as electron acceptor										
2400-1	$2NO_2^- + 2H^+ = 1.5O_2(aq) + N_2(aq) + H_2O$	H ₂ O to O ₂	NO ₂ ⁻ to N ₂ (aq)	3[1]-[24]	6	-3156,230	-1,400	83674,8	1318,37	6,0048,E-04
2400-2	$3H_2(aq) + 2NO_2^- + 2H^+ = N_2(aq) + 4H_2O$	H ₂ to H ⁺	NO ₂ ⁻ to N ₂ (aq)	3[2]-[24]	6	-1455,580	-0,683	83236,5	611,97	3,0186,E-04
2400-5	$3H_2S(aq) + 8NO_2^- + 2H^+ = 3SO_4^{2-} + 4N_2(aq) + 4H_2O$	H ₂ S to SO ₄	NO ₂ ⁻ to N ₂ (aq)	3[5]-4[24]	24	-3266,151	-1,446	233592,1	1351,44	6,1273,E-04
2400-21	$3NH_4^+ + 8NO_2^- + 2H^+ = 3NO_3^- + 4N_2(aq) + 7H_2O$	NH ₄ to NO ₃	NO ₂ ⁻ to N ₂ (aq)	3[21]-4[24]	24	-6895,932	-3,071	244633,1	2878,45	1,3251,E-03
2400-22	$NH_4^+ + NO_2^- = N_2(aq) + 2H_2O$	NH ₄ to NO ₂	NO ₂ ⁻ to N ₂ (aq)	[22]-[24]	6	-1479,620	-0,655	54645,5	617,08	2,8266,E-04
2400-23	$2NH_4^+ + 2NO_2^- = 2N_2(aq) + 4H_2O$	NH ₄ to N ₂	NO ₂ ⁻ to N ₂ (aq)	[23]-[24]	6	-2962,136	-1,312	109368,0	1235,34	5,6570,E-04
2400-24	$10NO_2^- + 4H^+ = 6NO_3^- + 2N_2(aq) + 2H_2O$	N ₂ to NO ₃	NO ₂ ⁻ to N ₂ (aq)	3[25]-5[24]	30	-4855,021	-2,187	159811,3	2030,23	9,4614,E-04
2400-25	$5NO_2^- + 2H^+ = 3NO_3^- + N_2(aq) + H_2O$	NO ₂ to NO ₃	NO ₂ ⁻ to N ₂ (aq)	3[26]-[24]	6	-2453,470	-1,104	80583,4	1025,80	4,7687,E-04
$2NO_3^- + 12H^+ + 10e^- = N_{2(aq)} + 6H_2O$ half reaction as electron acceptor										
2500-1	$2NO_3^- + 2H^+ = 2.5O_2(aq) + N_2(aq) + H_2O$	H ₂ O to O ₂	NO ₃ ⁻ to N ₂ (aq)	5[1]-[25]	10	-3642,0433	-1,6040	86187,5	1520,54	6,8542,E-04
2500-2	$5H_2(aq) + 2NO_3^- + 2H^+ = N_2(aq) + 6H_2O$	H ₂ to H ⁺	NO ₃ ⁻ to N ₂ (aq)	5[2]-[25]	10	-807,6267	-0,4097	85457,1	343,21	1,8772,E-04
2500-5	$5H_2S(s) + 8NO_3^- = 5SO_4^{2-} + 2H^+ + 4N_2(aq) + 4H_2O$	H ₂ S to SO ₄	NO ₃ ⁻ to N ₂ (aq)	5[5]-4[25]	40	1029,7767	0,5064	176238,5	-454,58	-2,4030,E-04
2500-21	$5NH_4^+ + 3NO_3^- = 2H^+ + 4N_2(aq) + 9H_2O$	NH ₄ to NO ₃	NO ₃ ⁻ to N ₂ (aq)	5[21]-4[25]	40	-5019,8588	-2,2020	194640,1	2090,44	9,4699,E-04
2500-22	$5NH_4^+ + 6NO_3^- = 5NO_2^- + 4H^+ + 3N_2(aq) + 8H_2O$	NH ₄ to NO ₂	NO ₃ ⁻ to N ₂ (aq)	5[22]-3[25]	30	-2543,0790	-1,0896	113416,0	1055,15	4,6717,E-04
2500-23	$10NH_4^+ + 6NO_3^- = 8N_2(aq) + 4H^+ + 18H_2O$	NH ₄ to N ₂	NO ₃ ⁻ to N ₂ (aq)	5[23]-3[25]	30	-9955,6612	-4,3715	387028,5	4146,45	1,8824,E-03
2500-24	$2N_2(aq) + 2H_2O + 6NO_3^- = 10NO_2^- + 4H^+$	N ₂ to NO ₂	NO ₃ ⁻ to N ₂ (aq)	5[24]-3[25]	30	4855,0212	2,1868	-159811,3	-2030,23	-9,4614,E-04
2500-25	$5NO_2^- + 2H^+ = 3NO_3^- + N_2(aq) + H_2O$	NO ₂ to NO ₃	NO ₃ ⁻ to N ₂ (aq)	5[26]-[25]	10	-2470,7763	-1,1107	81035,3	1032,93	4,7940,E-04
$NO_3^- + 2H^+ + 2e^- = NO_2^- + H_2O$ as electron acceptor										
2600-1	$NO_3^- = 0.5O_2(aq) + NO_2^-$	H ₂ O to O ₂	NO ₃ ⁻ to NO ₂ ⁻	[1]-[26]	2	-234,253	-0,0987	1030,4	97,52	4,1203,E-05
2600-2	$H_2(aq) + NO_3^- = NO_2^- + H_2O$	H ₂ to H ⁺	NO ₃ ⁻ to NO ₂ ⁻	[2]-[26]	2	332,630	0,1402	884,4	-137,94	-5,8337,E-05
2600-5	$H_2S(aq) + 4NO_3^- = SO_4^{2-} + 2H^+ + 4NO_2^-$	H ₂ S to SO ₄	NO ₃ ⁻ to NO ₂ ⁻	[5]-4[26]	8	2182,576	0,9898	-29580,5	-917,26	-4,3158,E-04
2600-21	$NH_4^+ + 3NO_3^- = 2H^+ + 4NO_2^- + H_2O$	NH ₄ to NO ₃	NO ₃ ⁻ to NO ₂ ⁻	[21]-4[26]	8	972,649	0,4482	-25900,2	-408,26	-1,9412,E-04
2600-22	$NH_4^+ + 3NO_3^- = 4NO_2^- + 2H^+ + H_2O$	NH ₄ to NO ₂	NO ₃ ⁻ to NO ₂ ⁻	[22]-3[26]	6	973,850	0,4485	-25938,0	-408,73	-1,9421,E-04
2600-23	$2NH_4^+ + 3NO_3^- = N_2(aq) + 2H^+ + 3NO_2^- + 3H_2O$	NH ₄ to N ₂	NO ₃ ⁻ to NO ₂ ⁻	[23]-3[26]	6	-508,666	-0,2079	28784,5	209,53	8,8834,E-05
2600-24	$N_2(aq) + H_2O + 3NO_3^- = 5NO_2^- + 2H^+$	N ₂ to NO ₂	NO ₃ ⁻ to NO ₂ ⁻	[24]-3[26]	6	2453,470	1,1038	-80583,4	-1025,80	-4,7687,E-04
2600-25	$N_2(aq) + H_2O + 3NO_3^- = 5NO_2^- + 2H^+$	N ₂ to NO ₃	NO ₃ ⁻ to NO ₂ ⁻	[25]-5[26]	10	2470,776	1,1107	-81035,3	-1032,93	-4,7940,E-04

3 Chemical composition of the water samples collected

3.1 Major elements

The major elemental composition of the water samples is given in Table 5. The waters had temperatures of 2-125°C, pH of 2.48-9.72 and total dissolved solids between 0.8 and 31.6 mmol/L (Fig. 3).

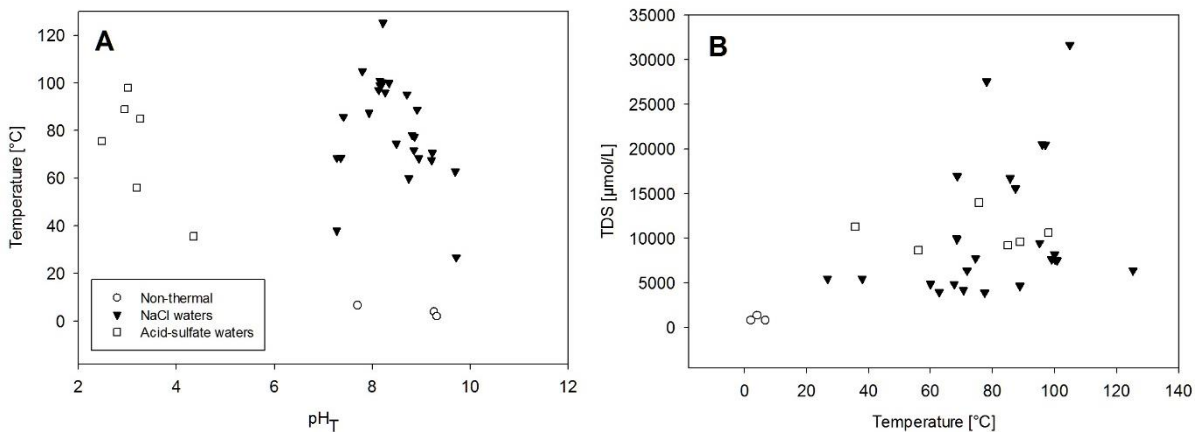


Figure 3 A) The relationship between *in situ* pH and temperature in all samples showing the differences between non-thermal waters (open circles), NaCl waters (black triangles) and acid-sulfate waters (open squares) and B) The relationship between temperature and total dissolved solids. The legends are the same as in A.

Based on the major cation and anion composition and temperature, the samples were divided into three categories: (1) NaCl waters, (2) acid-sulfate waters and (3) non-thermal waters (Fig 4). NaCl water samples were discharged by hot springs and wells with elevated pH of 7.27-9.72 and temperatures of 27-125°C. NaCl waters had neutral to alkaline pH values and elevated Cl concentrations up to 13893 μmol/L. Other dominant elements included Si (637-5991 μmol/L), Na (1959-13347 μmol/L), CO₂ (62-8223 μmol/L) and SO₄ (36-1016 μmol/L) (Table 5). The pH of the acid-sulfate waters varied between 2.48 and 4.35. The waters contained higher concentrations of SO₄ (3341-6582 μmol/L) and Fe (up to 361 μmol/L) Mg (up to 899 μmol/L) and Al (up to 1421 μmol/L). Non-thermal waters were mainly categorized by their low temperatures (<10°C) but they were also characterized by low concentrations of dissolved elements.

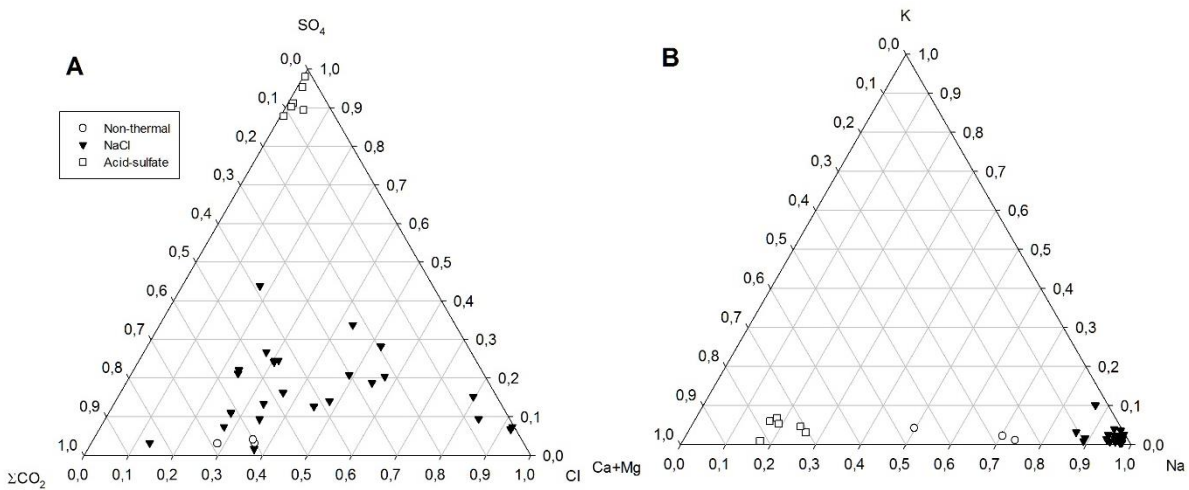


Figure 4 The distribution of A) ΣCO_2 - SO_4 - Cl and B) $\text{Ca}+\text{Mg}$ - K - Na for natural waters in Iceland. These triangle plots are used to categorize the waters. Steam-heated acid-sulfate waters are distinctive in both plots. The legends are the same as in Figure 3.

3.2 Nitrogen compounds

Total nitrogen concentrations ranged from 3.67-637.22 $\mu\text{mol/L}$, decreasing with pH. Nitrogen species analyzed included: $\text{N}_{2(\text{aq})}$, NO_3^- , NO_2^- , $\text{N}_{\text{residual}}$ and $\sum\text{NH}_4^+$. Here, the $\sum\text{NH}_4^+$ indicates the sum of the concentrations of all dissolved N(-III) species. Total oxidized nitrogen concentrations were also measured, making it possible to calculate residual nitrogen, taken to represent organically derived N (N_{org}). The concentrations and concentration ratios of various nitrogen compounds are shown in Figures 5 and 6.

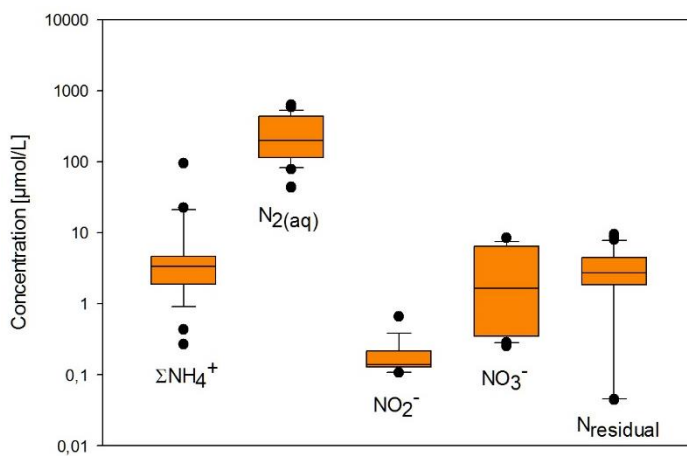


Figure 5 The distribution of nitrogen species in geothermal waters in Iceland.

Dissolved aqueous N_2 was detected in 26 out of 34 samples with concentrations of 44-634 $\mu\text{mol/L}$ and was usually the most abundant species accounting for 94-100% of all nitrogen species in alkaline waters and just under 90% in most steam heated acid-sulfate waters. After $\text{N}_{2(\text{aq})}$, $\sum\text{NH}_4^+$ and N_{org} were the most abundant oxidation states with NO_2^- and NO_3^- in even lower concentrations. No apparent trends with temperatures were observed, but concentrations of $\text{N}_{2(\text{aq})}$ increased with increasing pH. Ammonium was detected in all

samples with concentrations ranging from <0.1 to 95 $\mu\text{mol/L}$. Concentrations of NO_2 and NO_3^- were <0.1-0.66 $\mu\text{mol/L}$ and <0.1-8.51 $\mu\text{mol/L}$, respectively (Table 5). Organic nitrogen concentrations varied from 0 to 9.44 $\mu\text{mol/L}$. In acid-sulfate waters, $\sum\text{NH}_4^+$ and NO_3^- were the most abundant species with no N_{org} detected.

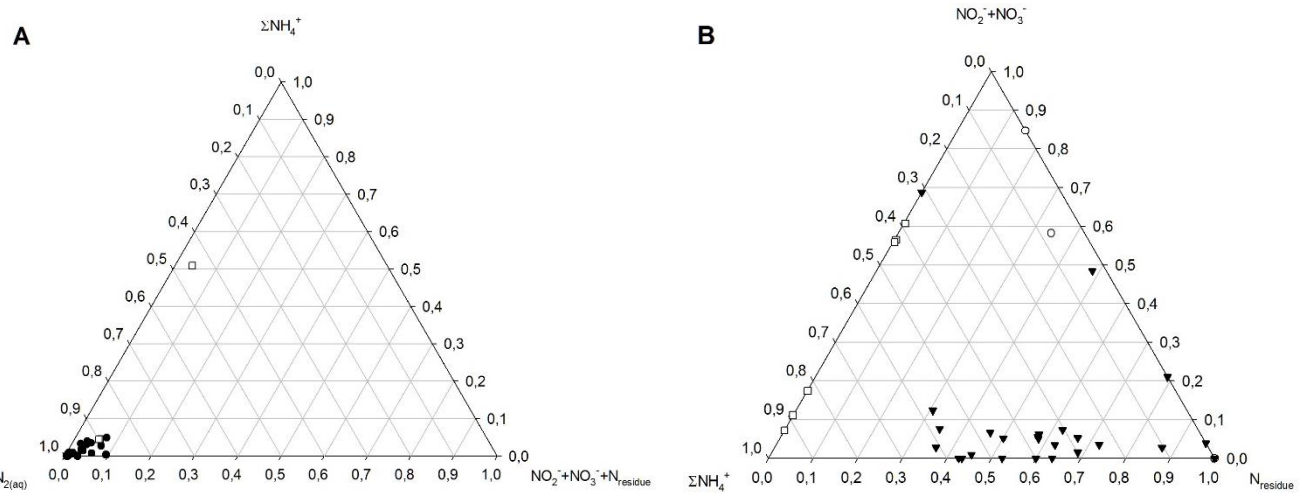


Figure 6 The distribution of A) $\text{N}_2\text{-NH}_4^-\text{-NO}_2^-+\text{NO}_3^-+\text{N}_{\text{residual}}$ and B) $\text{NH}_4^-\text{-NO}_2^-+\text{NO}_3^--\text{N}_{\text{residual}}$. Symbols have the same notations as Figure 4. These triangle plots, as well as the boxplot in Figure 5, are used to determine nitrogen species of importance. As can be seen in Figure A, the most important species is N_2 .

Table 5 Chemical composition of major elements, dissolved gases and nutrients in geothermal water, Iceland. Units are in $\mu\text{mol/L}$.

#	Location	Type	t°C	pH	/ °C	pH _T	Si	B	Na	K	Ca	Mg	Fe	Al	F	Cl
14-RSA-1	Hveragerði	Hot spring	69	7,44	/ 22	7,27	2993	24	4784	130	173	17,2	<0,01	0,77	67	1189
14-RSA-2	Ingólfssjall	Cold water	4	8,98	/ 22	9,26	236	<1	583	10	163	36,1	<0,01	0,30	5,0	279
14-RSA-3	Laugarbakkar	Well	60	9,23	/ 22	8,74	1045	19	2752	16	57	0,69	<0,01	0,91	30	793
14-RSA-4	Laugarvatn	Hot spring	100	9,29	/ 22	8,34	3009	9,2	3442	85	87	1,10	0,593	2,49	152	977
14-RSA-5	Vellankatla	Cold water	2	8,98	/ 22	9,32	240	<1	279	9	74	34,6	<0,01	0,61	4,4	128
14-RSA-6	Sísjódandi	Hot spring	96	9,10	/ 15	8,26	5432	90	9831	268	24	1,84	0,185	6,78	586	3245
14-RSA-7	Ótherrhíðar	Hot spring	97	8,87	/ 23	8,13	5991	89	9358	361	42	0,47	0,168	5,30	505	3181
14-RSA-8	Haukadalur	Hot spring	38	7,39	/ 17	7,27	1576	17	2461	92	202	97,3	0,761	<0,20	57	726
14-RSA-9	Nedridalur	Well	69	7,46	/ 29	7,36	3480	33	10035	1166	279	43,2	0,574	0,28	279	1282
14-RSA-10	Lyngdalsheiði	Cold water	7	7,57	/ 22	7,70	255	<1	186	16	104	68,3	0,136	<0,20	4,2	124
14-RSA-11	Marteinslaug	Hot spring	86	7,66	/ 22	7,41	5178	68	7558	324	131	6,34	<0,01	1,40	249	2484
14-RSA-12	Vadmálahver	Hot spring	99	9,05	/ 22	8,16	2521	36	3607	57	48	0,34	0,092	5,67	75	707
14-RSA-13	Flúdir	Well	100	9,12	/ 22	8,21	2504	35	3574	57	47	0,34	<0,01	5,92	76	720
14-RSA-14	Flúdir	Well	101	9,06	/ 22	8,15	2576	32	3489	58	35	0,25	0,094	4,05	74	684
14-RSA-15	Sólheimar	Well	87	8,72	/ 22	7,93	1701	18	6976	107	347	0,84	<0,01	1,00	102	5690
14-RSA-16	Oddgeirshíðar	Well	78	9,66	/ 21	8,82	1151	14	11952	121	1354	<0,20	<0,01	2,09	32	11968
14-RSA-17	Reykhóll	Well	68	9,65	/ 22	8,95	1180	17	4804	40	215	<0,20	<0,01	1,80	141	2990
14-RSA-18	Sóleyjarbakki	Well	27	9,79	/ 22	9,72	637	12	3048	18	52	0,63	0,144	0,61	79	1198
14-RSA-19	Bergsstadir	Well	95	9,65	/ 22	8,70	2236	44	4695	58	71	0,90	0,720	8,45	103	1402
14-RSA-20	Spóastadir	Well	75	9,16	/ 22	8,49	1728	27	3733	49	99	0,32	<0,01	1,12	149	1361
14-RSA-21	Húnavellir (well 21)	Well	72	9,56	/ 20	8,85	1834	2,1	3184	52	94	2,38	<0,01	0,88	264	263
14-RSA-22	Siglufjördur (well 11)	Well	71	10,00	/ 21	9,23	1669	3,1	2062	20	40	<0,20	<0,01	2,86	19	251
14-RSA-23	Borgarmýrar	Well	68	9,94	/ 23	9,21	1197	15	2520	19	82	<0,20	0,101	2,77	78	520
14-RSA-24	Laugarin Reykjadalur	Well	63	10,58	/ 21	9,69	1298	4,7	2262	13	51	<0,20	<0,01	12,55	38	141
14-RSA-25	Hveravellir	Well	125	9,37	/ 22	8,22	2963	6,3	2601	65	44	<0,20	<0,01	8,43	46	326
14-RSA-26	Reykir in Fnjóskadalur	Well	89	9,87	/ 22	8,92	1857	7,7	2157	25	43	<0,20	0,169	9,56	22	201
14-RSA-28	Bakki II	Well	105	8,76	/ 22	7,80	1660	18	13347	264	1395	0,76	0,100	1,61	24	13893
14-RSA-29	Mosfellsdalur	Well	77	9,66	/ 22	8,86	1172	3,5	1959	19	59	<0,20	0,097	5,59	30	446
14-RSA-30	Hveragerði	Hot spring	98	2,53	/ 22	3,01	2828	13	239	14	636	503	222	1271	13	215
14-RSA-31	Hveragerði	Hot spring	56	2,67	/ 22	3,19	2800	10	172	65	322	399	159	1276	14	43
14-RSA-32	Hveragerði	Hot spring	85	2,57	/ 22	3,26	2972	11	166	59	335	428	161	1421	13	32
14-RSA-33	Hveragerði	Hot spring	36	2,78	/ 22	4,35	3142	11	474	133	962	899	92,6	1374	12	58
14-RSA-34	Hveragerði	Hot spring	89	3,82	/ 22	2,94	2272	5,6	642	76	1729	<0,20	9,34	561	10	54
14-RSA-37	Hveragerði	Hot spring	76	2,25	/ 22	2,48	4377	10	298	57	403	467	361	1312	13	34

Table 5 continued

#	H ₂ S	SO ₄	ΣCO ₂	DOC	NH ₄	N ₂	NO ₂	NO ₃	N _{residue}	H ₂	O ₂	IB%
14-RSA-1	45	477	2674	50	1,0	131	<0.05	0,25	8,06	1,70	0,76	5,7
14-RSA-2	<0.3	24	459	24	<0.25		<0.05	8,51	1,54			7,6
14-RSA-3	19	36	1303	116	3,9	253	0,20	<0.25	8,95	0,25	0,01	6,8
14-RSA-4	30	349	384	46	4,1		0,17	0,73	2,21			12,4
14-RSA-5	<0.3	15	215	12	0,4		<0.05	3,37	1,99			9,2
14-RSA-6	68	955	2572	58	3,4	589	0,31	0,51	6,93	<0.01	131,43	4,1
14-RSA-7	70	891	2975	41	4,0	130	0,25	0,50	9,44	<0.01	1,97	2,5
14-RSA-8	<0.3	194	1706	39	0,3	78	<0.05	4,09	4,09	0,02	13,50	7,2
14-RSA-9	<0.3	321	8223	40	<0.25	249	<0.05	<0.25	7,65	<0.01	29,77	8,8
14-RSA-10	<0.3	14	300	27	<0.25		<0.05	<0.25	3,67			10,8
14-RSA-11	30	676	4020	33	6,4	153	0,11	<0.25	5,35	<0.01	5,77	1,0
14-RSA-12	62	571	1045	25	3,5	104	0,11	0,38	3,41	0,12	2,71	4,7
14-RSA-13	62	565	1019	26	3,0		0,13	0,28	4,69			3,8
14-RSA-14	56	542	1019	33	2,8	156	0,13	0,35	4,42	<0.01	6,08	4,3
14-RSA-15	17	643	471	33	2,9	419	<0.05	<0.25	2,26	0,34	4,81	0,5
14-RSA-16	1,3	954	62	27	3,6	438	<0.05	<0.25	2,70	<0.01	3,26	0,8
14-RSA-17	10	572	199	19	1,9	242	<0.05	0,28	2,95	0,70	3,23	2,5
14-RSA-18	7,6	407	568	20	1,9	447	<0.05	<0.25	3,35	<0.01	6,40	0,3
14-RSA-19	37	756	520	66	4,4	115	0,16	0,35	4,92	<0.01	3,14	3,4
14-RSA-20	16	581	839	29	2,4	44	<0.05	<0.25	3,62	<0.01	2,49	1,2
14-RSA-21	40	662	584	17	<0.25	503	0,14	<0.25	3,46	0,02	3,80	4,3
14-RSA-22	15	100	397	35	<0.25	634	0,66	<0.25	2,49	<0.01	11,69	4,0
14-RSA-23	12	406	276	<10	1,3	157	0,13	<0.25	2,37	<0.01	2,31	3,7
14-RSA-24	<0.3	138	236	16	1,2	472	0,22	2,54	0,00	0,63	2,97	3,7
14-RSA-25	41	307	751	11	3,3	355	0,14	0,29	1,96	0,65	2,67	3,9
14-RSA-26	3,1	178	461	155	0,9	329	0,13	<0.25	2,73	1,67	2,31	3,2
14-RSA-28	10	1016	173	19	4,6	134	0,21	<0.25	2,74	0,00	0,68	0,3
14-RSA-29	13	198	578	15	2,0	502	<0.05	<0.25	2,24	0,22	0,19	1,8
14-RSA-30	<0.3	4368	302	204	95	84	<0.05	7,45	0,10	<0.01	13,37	-0,2
14-RSA-31	<0.3	3341	280	41	5,7	113	<0.05	7,45	0,06	<0.01	24,43	0,0
14-RSA-32	<0.3	3537	460	43	5,5	112	<0.05	7,08	0,06	<0.01	23,39	-0,1
14-RSA-33	<0.3	4073	383	41	21		<0.05	4,47	0,05			-0,2
14-RSA-34	<0.3	4146	150	55	23		0,11	2,75	0,00			-0,1
14-RSA-37	<0.3	6582	97	91	4,7		<0.05	7,33	0,04			0,1

4 Discussion

4.1 Aqueous speciation of nitrogen compounds

The results of speciation calculations for nitrogen compounds can be found in Figure 7. These calculations were carried out with the aid of the PHREEQC program and the llnl.dat database (Parkhurst and Appelo, 1999) based on chemical analysis of the various nitrogen oxidation states given in Table 5. The outcome of these calculations largely depends on the thermodynamic database used.

To study the speciation of nitrogen, different oxidation states were observed; N_2 , NO_3^- , NO_2^- , $\sum\text{NH}_4^+$ and $\text{N}_{\text{organic}}$. The distribution of nitrogen oxidation states can be found in Figure 6. For $\sum\text{NH}_4^+$ that the dominant species was found to be NH_4^+ at low pH and low temperatures i.e. in acid-sulfate waters, where $\text{NH}_3(\text{aq})$ was the dominant species under neutral to alkaline pH conditions and at high temperatures, i.e. in NaCl type waters, but NH_4SO_4 species was not found to predominate (Figure 7a). Nitrate and nitrite were also found to be important and dominating species over HNO_3 and HNO_2 (Figure 7b and 7c). Other species, such as FeNO_2^{+2} and FeNO_3^{+2} , were considered to be less important.

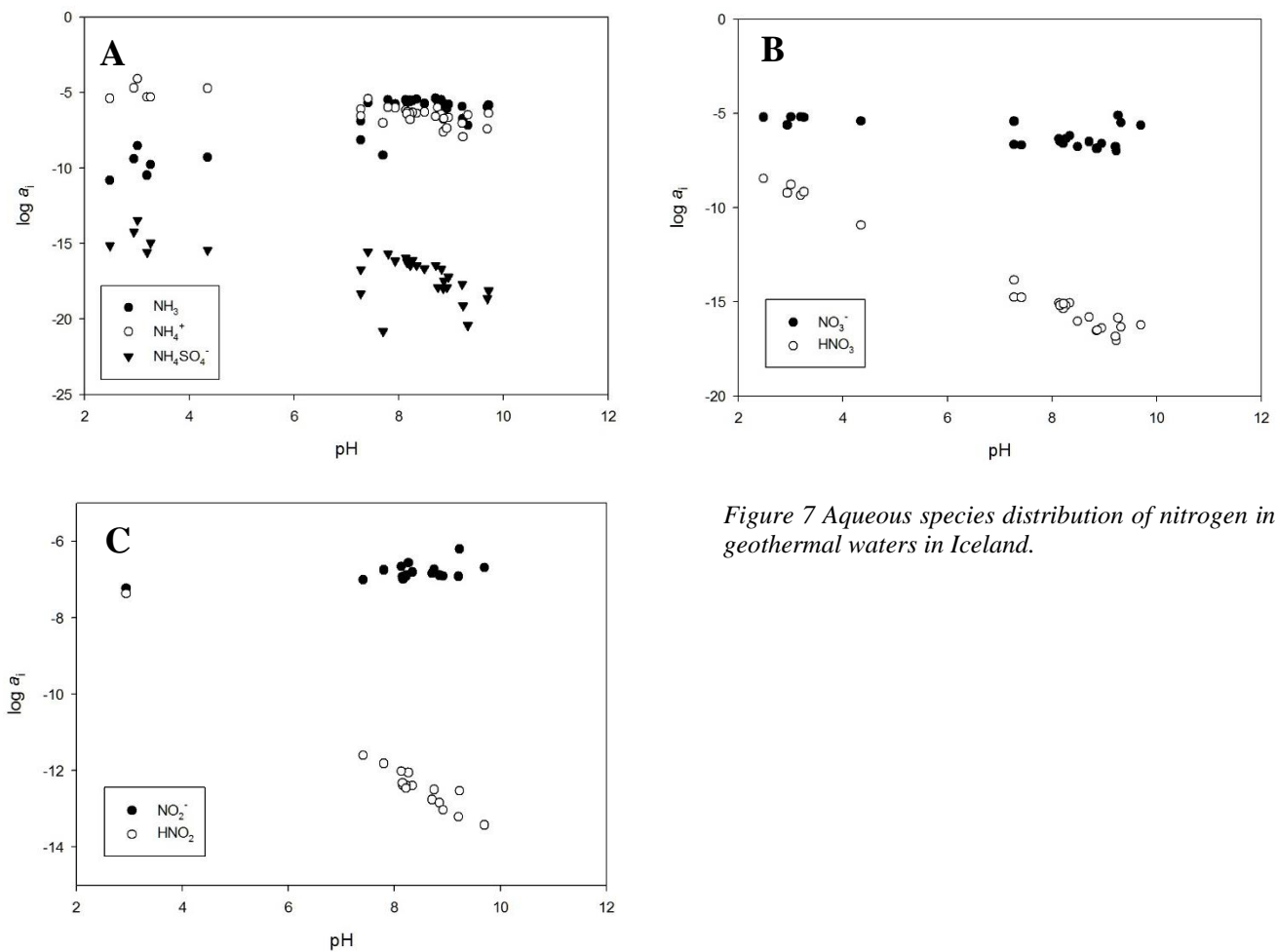


Figure 7 Aqueous species distribution of nitrogen in geothermal waters in Iceland.

4.2 Electron potential and half redox reactions

The oxidation states of nitrogen in geothermal fluids range from N(-III) to N(+V). Reactions between the various oxidation states of nitrogen may be studied by calculating and comparing the various redox potentials for given redox pairs.

The redox potential may be defined in terms of the electron potential (pe) for a particular half redox reaction,

$$\text{pe} = -\log a_e \equiv \log Q - \log K$$

The redox pairs considered here were NH_4^+/N_2 , $\text{NH}_4^+/\text{NO}_2^-$, $\text{NH}_4^+/\text{NO}_3^-$, N_2/NO_2^- , N_2/NO_3^- and $\text{NO}_2^-/\text{NO}_3^-$ together with H_2/H^+ , $\text{H}_2\text{O}/\text{O}_2$ and $\text{H}_2\text{S}/\text{SO}_4^{2-}$ for comparison. The half reactions and the respective definition of pe are listed in Table 3 and the respective equilibrium constants are given in Table 2. The activities of the aqueous species involved in the calculations were calculated with the aid of the PHREEQC program (Parkhurst and Appelo, 1999) and are listed in Table 6. The resulting pe values are reported in Appendix A and shown in Figure 8.

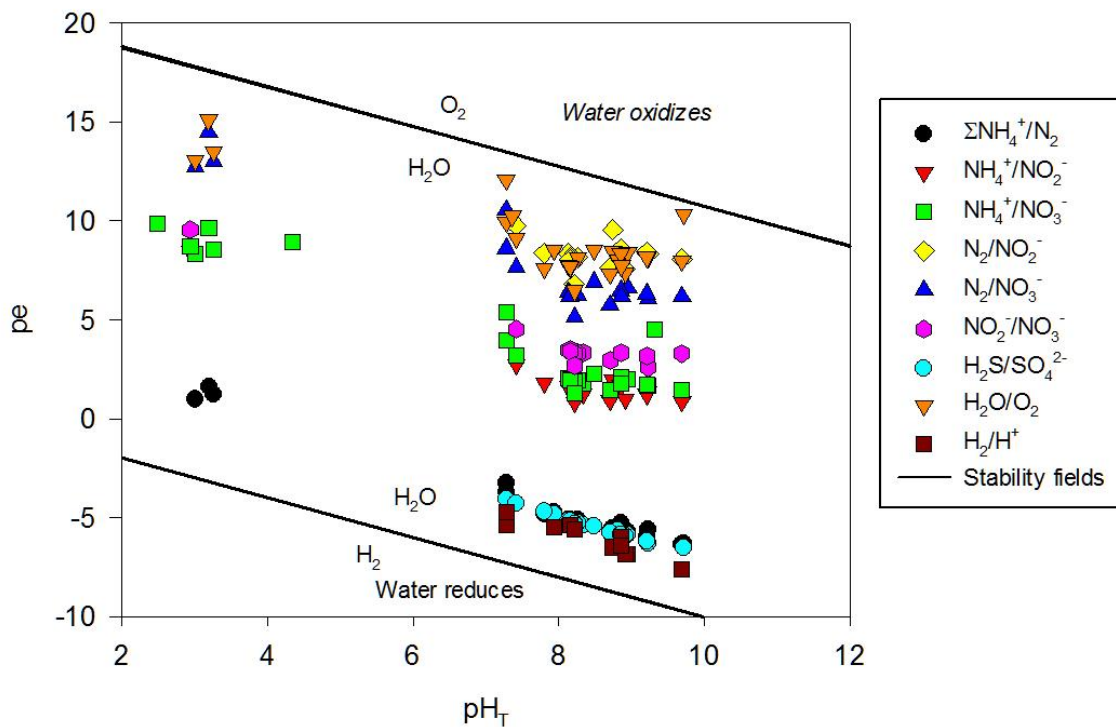


Figure 8 Calculated redox potentials for half reactions of interest.

For all water types, the pe values between the various half redox reactions differ by up to ~15 pe units for the nitrogen containing reactions. This indicates that overall redox equilibrium between the various nitrogen-containing reactions does not prevail in the waters in the current study. This is in agreement with previous work on redox disequilibrium in non-thermal and thermal waters at < 200°C (Linberg and Runnels, 1984; Stefánsson et al., 2005). According to Stefánsson et al. (2005) the redox chemistry of natural open aqueous systems are controlled by steady state between supply of the

elements to the system and the kinetics of reactions involving these elements, i.e. the source of nitrogen containing compounds and their reactions. However, the concentrations of various oxidation states of a given element may be controlled by equilibrium of kinetically fast reactions, whereas an overall redox equilibrium will not be reached until the system is completely closed.

A close inspection of the pe values (Table 6 and Figure 8) indicate that the half reaction between NH_4^+ and N_2 in our study is very close to that of H_2/H^+ and $\text{H}_2\text{S}/\text{SO}_4^{2-}$ redox pair. This may indicate closeness to equilibrium for these elements. For other redox couples involving nitrogen compounds, a much more oxidized conditions are observed and these being scattered by ~5-10 pe units, suggesting non-equilibrium conditions and either source controlled or kinetically controlled concentrations of NO_2^- and NO_3^- .

Table 6 Aqueous species activities

#	t°C	pH _T	loga _i								
			H ⁺	H ₂ (aq)	O ₂ (aq)	H ₂ S(aq)	SO ₄ ⁻²	N ₂ (aq)	NO ₂ ⁻	NO ₃ ⁻	NH ₄ ⁺
14-RSA-1	69	7,27	-7,27	-6,07	-6,42	-5,14	-3,49	-4,18		-6,64	-6,10
14-RSA-2	4	9,26	-9,26				-4,69			-5,09	
14-RSA-3	60	8,74	-8,74	-6,90	-8,30	-6,84	-4,56	-3,90	-6,73		-6,00
14-RSA-4	100	8,34	-8,34			-6,43	-3,60		-6,80	-6,17	-6,38
14-RSA-5	2	9,32	-9,32				-4,88			-5,48	-6,49
14-RSA-6	96	8,26	-8,26		-4,18	-6,01	-3,25	-3,53	-6,56	-6,35	-6,32
14-RSA-7	97	8,13	-8,13		-6,01	-5,87	-3,28	-4,19	-6,66	-6,36	-6,16
14-RSA-8	38	7,27	-7,27	-7,96	-5,17		-3,85	-4,41		-5,42	-6,56
14-RSA-9	69	7,36	-7,36		-4,83		-3,74	-3,90			
14-RSA-10	7	7,70	-7,70				-4,91				-7,02
14-RSA-11	86	7,41	-7,41		-5,54	-5,52	-3,38	-4,12	-7,01	-6,67	-5,41
14-RSA-12	99	8,16	-8,16	-7,23	-5,87	-5,94	-3,40	-4,28	-6,99	-6,46	-6,27
14-RSA-13	100	8,21	-8,21			-5,99	-3,40		-6,92	-6,59	-6,40
14-RSA-14	101	8,15	-8,15		-5,52	-5,98	-3,42	-4,11	-6,92	-6,49	-6,39
14-RSA-15	87	7,93	-7,93	-6,76	-5,62	-6,25	-3,41	-3,68			-6,01
14-RSA-16	78	8,82	-8,82		-5,79	-8,22	-3,33	-3,66			-6,45
14-RSA-17	68	8,95	-8,95	-6,46	-5,79	-7,39	-3,41	-3,92		-6,59	-6,64
14-RSA-18	27	9,72	-9,72		-5,49	-7,89	-3,51	-3,65			-6,38
14-RSA-19	95	8,70	-8,70		-5,80	-6,69	-3,29	-4,24	-6,84	-6,50	-6,58
14-RSA-20	75	8,49	-8,49		-5,90	-6,76	-3,39	-4,66		-6,76	-6,29
14-RSA-21	72	8,85	-8,85	-7,98	-5,72	-6,70	-3,32	-3,60	-6,89	-6,86	-7,61
14-RSA-22	71	9,23	-9,23		-5,23	-7,50	-4,11	-3,50	-6,21	-6,98	-7,93
14-RSA-23	68	9,21	-9,21		-5,94	-7,56	-3,52	-4,11	-6,92	-6,77	-7,04
14-RSA-24	63	9,69	-9,69	-6,50	-5,83		-3,97	-3,63	-6,68	-5,62	-7,42
14-RSA-25	125	8,22	-8,22	-6,49	-5,87	-6,20	-3,65	-3,75	-6,89	-6,57	-6,79
14-RSA-26	89	8,92	-8,92	-6,08	-5,94	-7,96	-3,86	-3,78	-6,91		-7,36
14-RSA-28	105	7,80	-7,80		-6,47	-6,43	-3,34	-4,17	-6,75		-5,97
14-RSA-29	77	8,86	-8,86	-6,96	-7,02	-7,22	-3,81	-3,60		-6,88	-6,72
14-RSA-30	98	3,01	-3,01		-5,17		-2,88	-4,38		-5,18	-4,08
14-RSA-31	56	3,19	-3,19		-4,91		-2,83	-4,25		-5,18	-5,29
14-RSA-32	85	3,26	-3,26		-4,93		-2,86	-4,25		-5,20	-5,31
14-RSA-33	36	4,35	-4,35				-2,72			-5,40	-4,73
14-RSA-34	89	2,94	-2,94				-2,84		-7,23	-5,62	-4,69
14-RSA-37	76	2,48	-2,48				-2,79			-5,20	-5,39

4.3 Overall redox reactions, reaction order and reaction energies

In order to study the possible overall redox reactions, the half reactions used to calculate the electron potentials were balanced against each other to give an overall redox reactions. These were further categorized into e⁻ accepting reaction. The overall reactions are listed in Table 4 and the results of the calculations (Q, K and affinity) are given in Appendices B to D and plotted in figures 9-17 as a function of pH and temperature. It should be noted that chemical affinity is reported as kcal/mol per e⁻ transfer instead of the more common saturation index (SI), the two linked through,

$$A_r \equiv RT\ln(K/Q) = -SI/RT$$

This unit is chosen to make it easier to compare reactions and systems to one another since energy of the reactions will be released as electrons are transferred. This means that when coupling various reactions together, the results are standardized to one mol of electrons. To make comparisons even easier, redox reactions were categorized to groups of electron acceptors. If affinity values are close to zero, or only a few calories above or below zero, there is insufficient or no available energy to drive the reaction. Somewhat higher affinities indicate that there are some disequilibrium energies available for driving the reaction. Large positive values mean that there is abundant energy available for the forward reaction whereas negative values indicate that there is energy available for the reaction written in the reverse direction.

O₂ to H₂O as electron acceptor (#100 reactions) - The reaction affinities where O₂ to H₂O is the electron acceptor reaction are plotted in Figure 9. As observed in Figure 9, almost all the reactions are negative with the positive energy values being low (< 2 kcal/mol e⁻ transferred). For this group of reactions, the sign of the slope is always negative and very similar between different reactions, except perhaps for a slightly positive result for the first reaction, and H⁺ is always the product. Some reactions (100-1 and 100-25) do not involve H⁺ but still follow a pH trend. This is explained by the fact that the chemical composition of geothermal waters change drastically with pH.

H⁺ to H₂ as electron acceptor (#200 reactions) - The reaction affinities where H⁺ (H₂O) to H₂ is the electron acceptor reaction are plotted in Figure 10. As observed, all reactions display positive energies suggesting that the reactions will proceed to the right. Many of the reactions display high energy release of > 10 kcal/mol e⁻ transferred.

SO₄²⁻ to H₂S as electron acceptor (#500 reactions) – The reaction affinities where SO₄²⁻ to H₂S is the electron acceptor reaction are plotted in Figure 11. Most of the reactions pose positive affinities indicating that the reactions will proceed to the right. Moreover, almost all the affinities increase with increasing pH. Many of the reactions display high-energy release of > 10 kcal/mol e⁻ transferred.

NO₃⁻ to NH₄⁺ as electron acceptor (#2100 reactions) – The reaction affinities where NO₃⁻ to NH₄⁺ is the electron acceptor reactions are plotted in Figure 12. The reactions poses both negative and positive values, but generally, as NO₃⁻ is being reduced to NH₄⁺, other N-containing species are oxidized including N₂ to NO₂⁻ and NO₃⁻ and NO₂⁻ to NO₃⁻.

NO₂⁻ to NH₄⁺ as electron acceptor (#2200 reactions) – The reaction affinities where NO₂⁻ to NH₄⁺ is the electron acceptor reaction are plotted in Figure 13. The reactions pose both positive and negative values. Relative to the N-compounds, as NO₂⁻ is being reduced to NH₄⁺, N₂ may be progressively oxidized to NO₂⁻ and NO₃⁻.

N₂ to NH₄⁺ as electron acceptor (#2300 reactions) – The reaction affinities where N₂ to NH₄⁺ is the electron acceptor reaction are plotted in Figure 14. The reactions pose both positive and negative values. Relative to the N-compounds, upon N₂ reduction to NH₄⁺, most other N-compounds oxidizes.

NO₂⁻ to N₂ as electron acceptor (#2400 reactions) – The reaction affinities where NO₂⁻ to N₂ is the electron acceptor, are plotted in Figure 15. All N-containing reactions have negative affinities relative to NO₂⁻ to N₂ reduction. This implies that this set of reactions are not feasible, instead, most N-containing compounds will be reduced upon N₂ to NO₂⁻ oxidation.

NO₃⁻ to N₂ as electron acceptor (#2500 reactions) – The reaction affinities where NO₃⁻ to N₂ is the electron acceptor are plotted in Figure 16. Almost all N-containing reactions proceed to the left relative to NO₃⁻ to N₂ reduction. This is similar to the previous reactions (#2400), i.e. most N-containing compounds will be reduced upon N₂ to NO₃⁻ oxidation.

NO₃⁻ to NO₂⁻ as electron acceptor (#2600 reactions) – The reaction affinities where NO₃⁻ to NO₂⁻ is the electron acceptor are plotted in Figure 17. Most of the reactions pose negative affinities, suggesting reduction upon NO₂⁻ to NO₃⁻ oxidation. The exception is N₂ to NO₂⁻ oxidation upon NO₃⁻ to NO₂⁻ reduction.

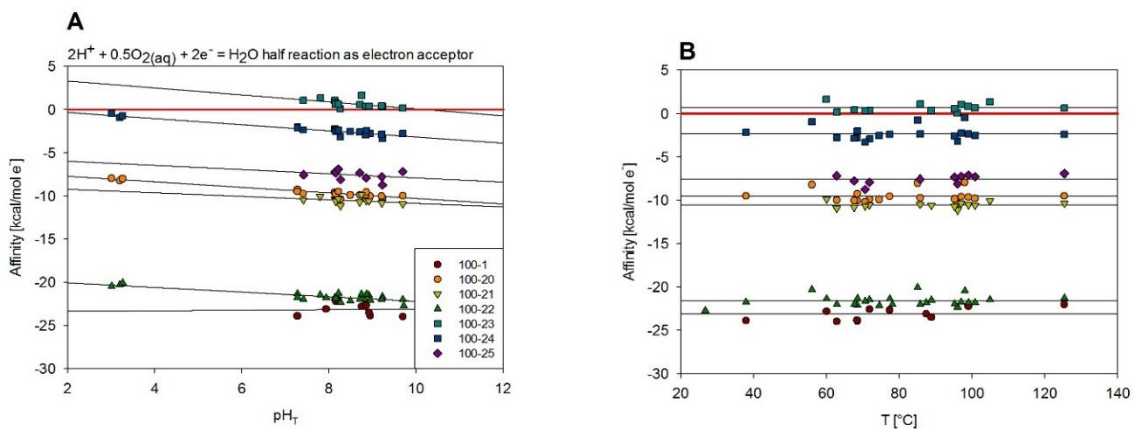


Figure 9 Affinities for reactions #100 ($2H^+ + 0.5O_{2(aq)} + 2e^- = H_2O$ half reaction as electron acceptor). The symbols in the figure represent the pH and temperature of each sample and their calculated affinities. The affinities are calculated from analytical data in Table 5 for the first set of reactions given in Table 4. The lines represent trends with each reaction given in Table 4.

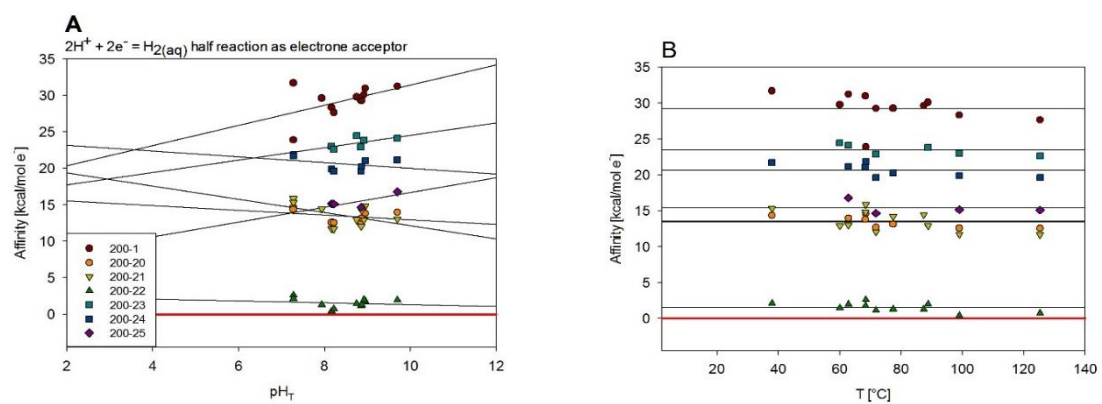


Figure 10 Affinities for reactions #200 ($2H^+ + 2e^- = H_2(aq)$ half reaction as electron acceptor) plotted with temperature and pH.

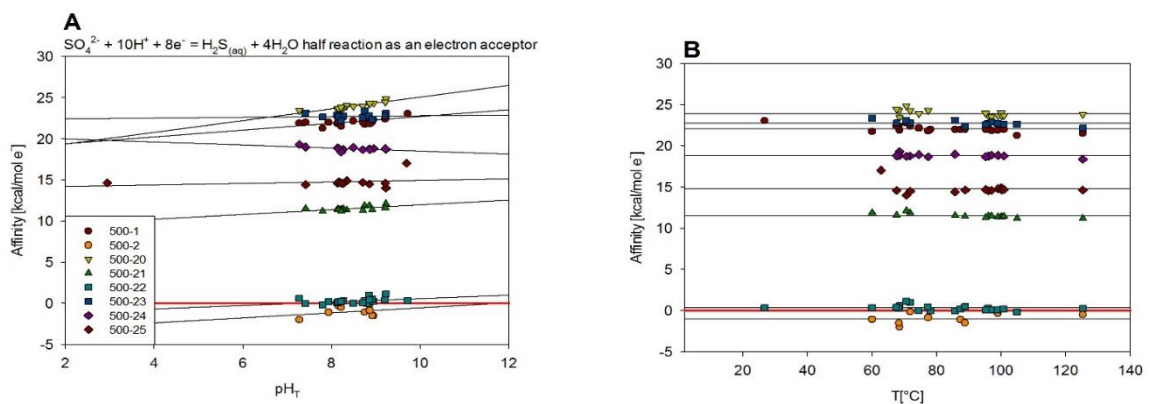


Figure 11 Affinities for reactions #500 ($SO_4^{2-} + 10H^+ + 8e^- = H_2S_{(aq)} + 4H_2O$ half reaction as an electron acceptor) plotted with temperature and pH.

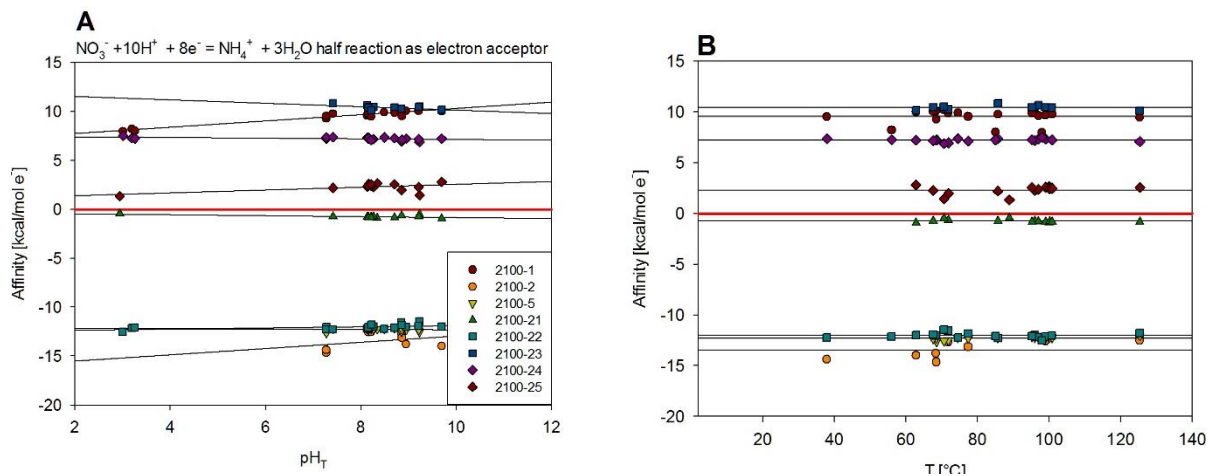


Figure 12 Affinities for reactions #2100 ($\text{NO}_3^- + 10\text{H}^+ + 8e^- = \text{NH}_4^+ + 3\text{H}_2\text{O}$ half reaction as electron acceptor) plotted with temperature and $p\text{H}$.

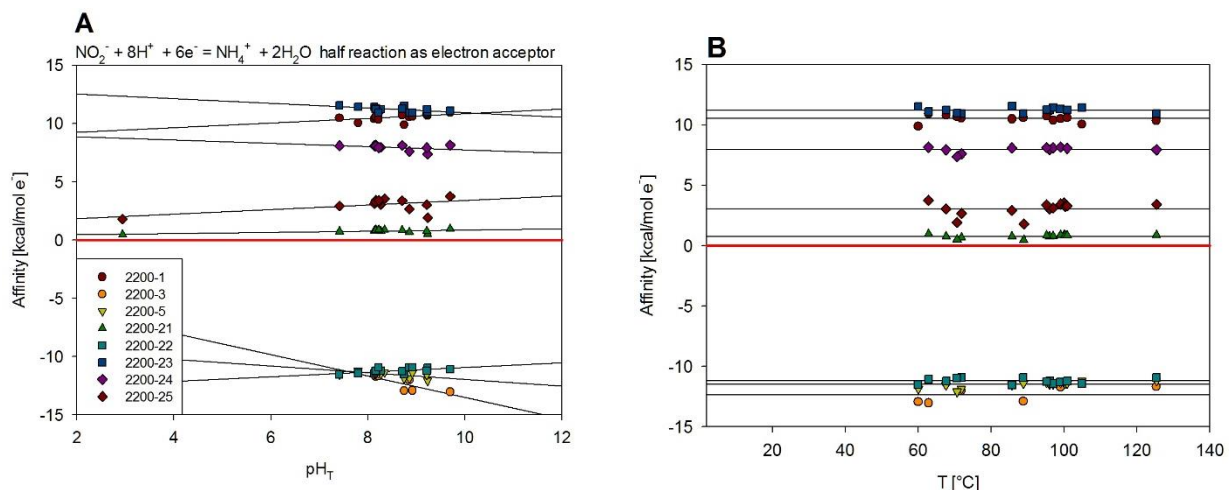


Figure 13 Affinities for reactions #2200 $\text{NO}_2^- + 8\text{H}^+ + 6e^- = \text{NH}_4^+ + 2\text{H}_2\text{O}$ half reaction as electron acceptor plotted with temperature and $p\text{H}$.

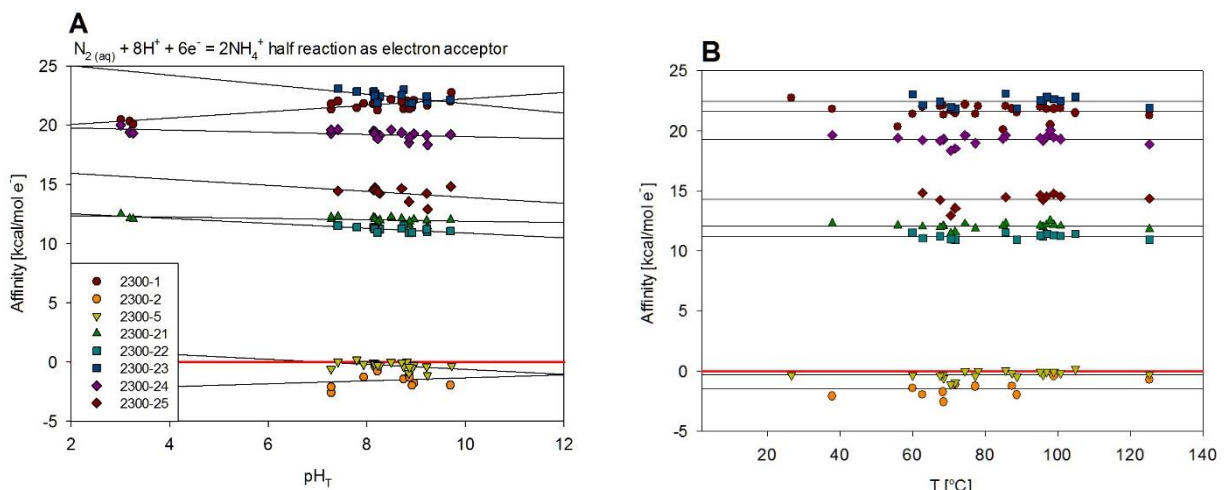


Figure 14 Affinities for reactions #2300 ($\text{N}_2(\text{aq}) + 8\text{H}^+ + 6e^- = 2\text{NH}_4^+$ half reaction as electron acceptor) plotted with temperature and $p\text{H}$.

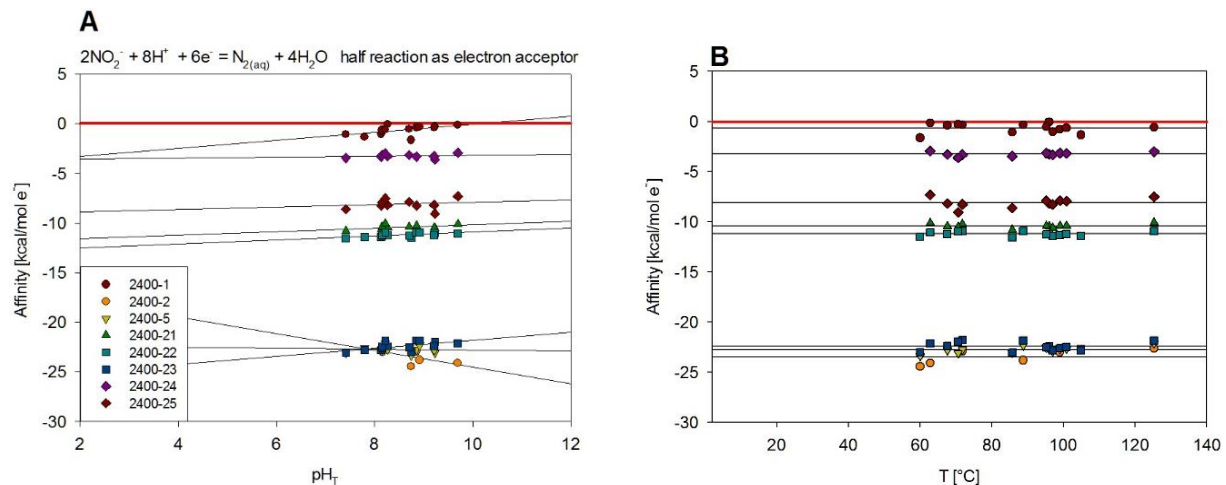


Figure 15 Affinities for reactions #2400 ($2\text{NO}_2^- + 8\text{H}^+ + 6e^- = \text{N}_{2(\text{aq})} + 4\text{H}_2\text{O}$ half reaction as electron acceptor) plotted with temperature and pH.

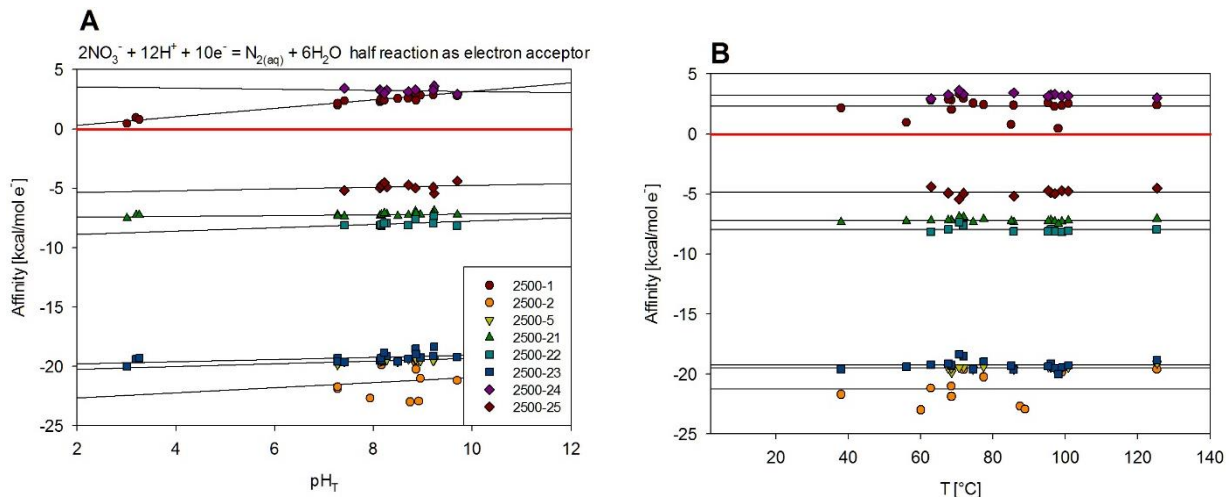


Figure 16 Affinities for reactions #2500 ($2\text{NO}_3^- + 12\text{H}^+ + 10e^- = \text{N}_{2(\text{aq})} + 6\text{H}_2\text{O}$ half reaction as electron acceptor) plotted with temperature and pH.

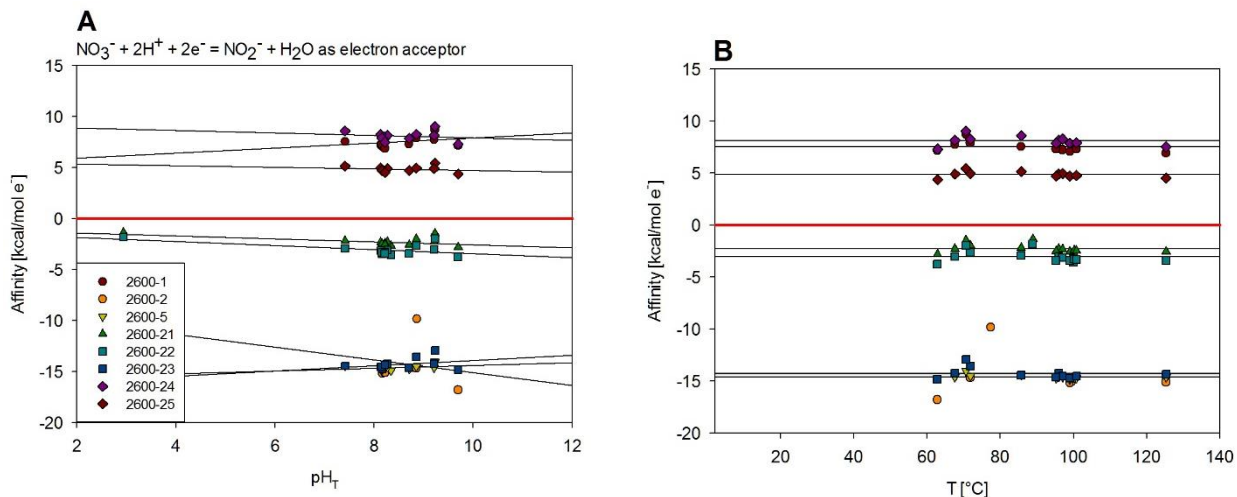
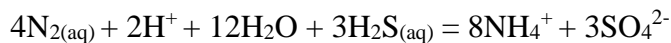


Figure 17 Affinities for reactions #2600 ($\text{NO}_3^- + 2\text{H}^+ + 2e^- = \text{NO}_2^- + \text{H}_2\text{O}$ as electron acceptor) plotted with temperature and pH.

Source and reactions of N-containing compounds

The source of various nitrogen compounds may be primarily two, firstly, from the fluid itself, and secondly, upon reactions occurring within the system. Possible nitrogen-redox reactions may be summarized into four groups: (i) nitrogen fixation where N_2 is being reduced to NH_4^+ , (ii) nitrification where NH_4^+ is being oxidized to NO_2^- and NO_3^- , (iii) denitrification where NO_3^- is being reduced eventually to N_2 and (iv) organic matter decomposition, for example the reduction of $\text{C}_{106}\text{N}_{16}\text{P}$ to NH_4^+ or oxidation of $\text{C}_{106}\text{N}_{16}\text{P}$ to NO_3^- .

Based on the reaction order and affinity calculations several possible N-containing reactions can be observed, including nitrogen fixation and nitrification. Nitrogen fixation applies to reduction of N_2 to NH_4^+ . Inspections of the calculated affinities reveal that nitrogen fixation by H_2 to H^+ and H_2S to SO_4^{2-} reduction according to the reactions,

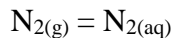


are very close to equilibrium with $A_r \sim 0$. This is also in accordance with the observation of similar electron potential (pe) for the half reactions H_2/H^+ , $\text{H}_2\text{S}/\text{SO}_4^{2-}$ and NH_4^+/N_2 .

The source of N_2 may be considered to be atmospheric and denitrification, i.e. the two major sources of N_2 assuming limited deep mantle N_2 source. Assuming the first, the air saturated $\text{N}_{2(\text{aq})}$ concentration may be calculated from,

$$m_{\text{N}_2(\text{aq})} = K_{\text{N}_2} p_{\text{N}_2(\text{g})}$$

where K_{N_2} is the equilibrium solubility of $\text{N}_{2(\text{g})}$ (Table 2) according to the reaction,



and is $p_{\text{N}_2(\text{g})}$ given by atmospheric pressure of $\text{N}_{2(\text{g})}$ taken to be 0.78 bar. The air saturated $\text{N}_{2(\text{aq})}$ concentration is compared with measured $\text{N}_{2(\text{aq})}$ concentration in Figure 18.

As observed, most waters are undersaturated with respect to atmospheric N_2 , suggesting a possible reduction of N_2 to NH_4^+ as discussed above. Addition of N_2 upon sampling and cooling of samples cannot explain this trend as the solubility decrease with increasing temperature to $\sim 100^\circ\text{C}$, such air contamination would result in too high N_2 concentration relative to equilibrium atmospheric concentration. The atmospheric source for N_2 is further supported by the N_2/Ar ratio, which is observed to lie between N_2/Ar ratio of air and N_2/Ar ratio of air saturated water (Fig. 18). Moreover, the decrease relative to air-saturated water is consistent with N_2 reduction to NH_4^+ as discussed above.

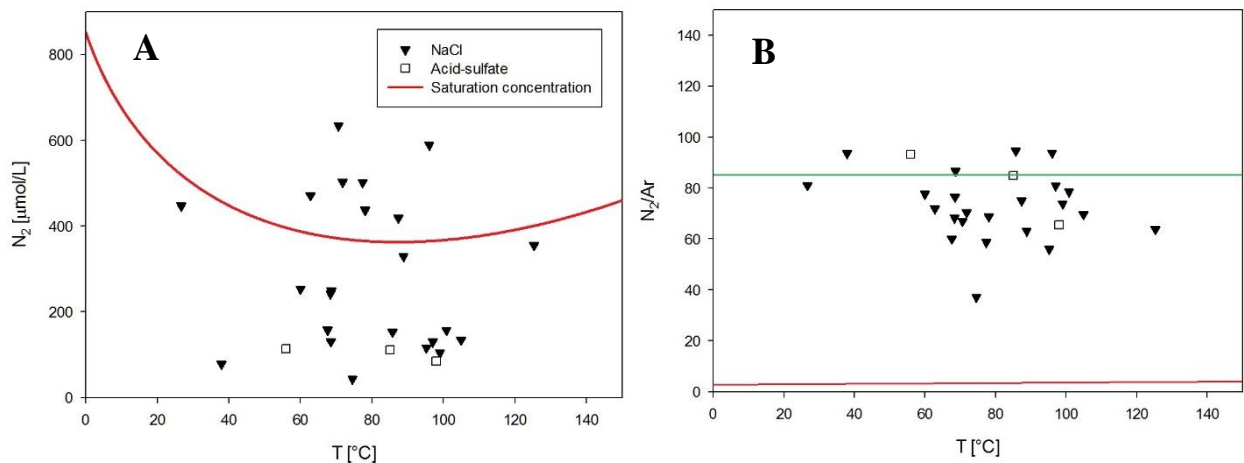
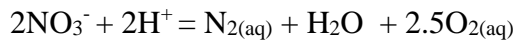


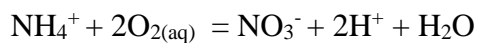
Figure 18 A) Concentrations of $N_2(aq)$ versus temperature compared with saturation line of N_2 in the atmosphere, and B) The ratio of N_2/Ar versus temperature showing that the samples plot between the lines of N_2/Ar ratios in air (green line) and the saturation line of N_2/Ar (red line), supporting that the source for N_2 is atmospheric.

Denitrification may also be a potential source of N_2 , i.e. reduction of NO_3^- to N_2 . This reaction is favored by oxidation of H_2O to O_2 according to the reaction,



Therefore, N_2 production upon NO_3^- reduction cannot be ruled out as a source of N_2 in the thermal waters. However, given the low concentration of NO_3^- in the thermal water sampled of <0.25-8.51 μmol/kg relative to the N_2 concentrations of 44-634 μmol/kg, or on average ~400 times greater, it is unlikely that the reduction of NO_3^- to N_2 in our study is a significant source of the latter. This leads to the conclusion that the source of N_2 in thermal water is most likely atmospheric and that ΣNH_4 is produced upon reduction of N_2 .

The source of NO_3 (and NO_2) in the thermal waters may be the result of nitrification, i.e. oxidation of NH_4^+ , for example according to the reactions



i.e. by reduction of O_2 to H_2O , H_2O to H_2 and/or SO_4^{2-} to H_2S . According to the results of the affinity calculations, the first reaction is unfavorable whereas the other two are favored, i.e. nitrification of NH_4^+ to NO_3^- may be caused by reduction of H_2O to H_2 and SO_4^{2-} to H_2S . Alternatively, disproportionation reactions involving nitrogen compounds may result in nitrification. Such reactions are very difficult to explore, as many possibilities are available. One possibility is simply oxidation of NH_4^+ to NO_3^- by the reduction of N_2 to NH_4^+ according to the reaction,



that is favorable according to the affinity calculations. In our results it is difficult to determine which of these reactions are the most important. However, such complex stoichiometry really needs to be assessed by observations in a controlled system upon reaction progress or reaction time in order to verify reactions and species with time.

The source of NO_3^- and NO_2^- may also be simply the source water, i.e. it does not produce upon reactions within the system. The source water of most thermal ground waters of low salinity in Iceland is meteoric (Árnason, 1976). The concentration of NO_3^- in rainwater in Iceland is 8.9 $\mu\text{mol/kg}$ (Gislason et al., 1996), that is somewhat higher than observed for most of the waters with values between <0.25-8.51 $\mu\text{mol/kg}$. Therefore, it cannot be ruled out that the source of NO_3^- and NO_2^- in the thermal waters could be the source water and that nitrification reactions do not really occur to any degree in the system.

Chlorine in the waters may be assumed to be derived from both marine source and rock dissolution. According to Arnórsson and Andrésdóttir (1995) the marine contribution of Cl may be calculated from the B and Cl relationship in the sampled waters and their respective ratios in rocks and seawater,

$$m_{\text{Cl}}^m = \frac{m_B - (B/\text{Cl})^r m_{\text{Cl}}}{(B/\text{Cl})^m - (B/\text{Cl})^r}$$

where m_{Cl}^m is the marine derived Cl, m_B and m_{Cl} is the measured B and Cl concentration, respectively, $(B/\text{Cl})^r$ and $(B/\text{Cl})^m$ are the B to Cl rock and Cl marine ratios taken to be 1/1330 and 1/30, respectively. Figure 19 shows the relationship between marine Cl (m_{Cl}^m) and measured NO_3^- and NO_2^- concentration. As observed in our study, no relationship between marine derived Cl and NO_3^- and NO_2^- concentrations prevails, possibly suggesting that the source of NO_3^- and NO_2^- in the water samples is not the source water, i.e. meteoric water.

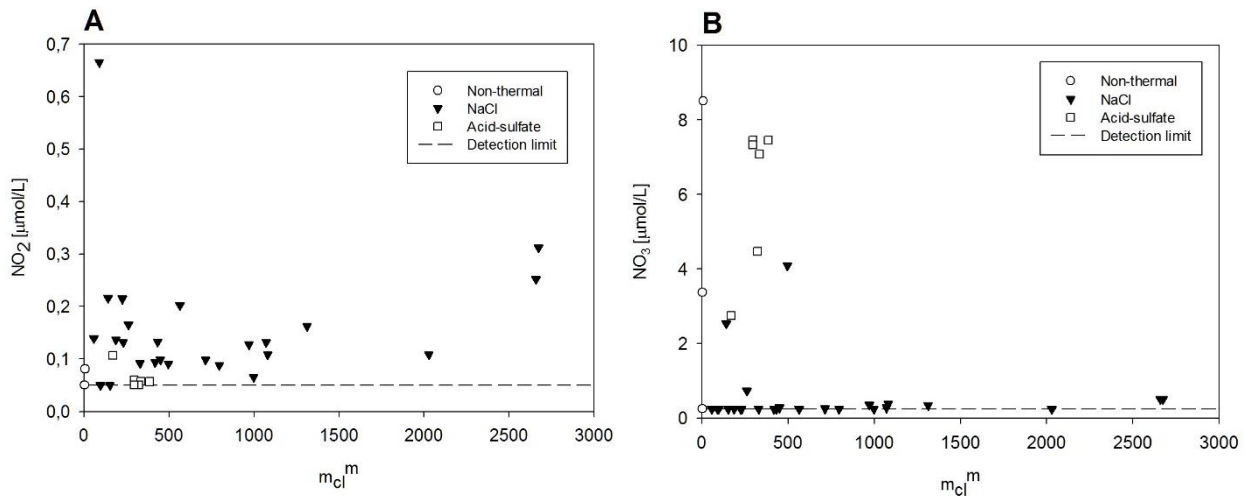


Figure 19 The relationship between marine Cl (m_{Cl}^m) and measured NO_3^- and NO_2^- concentration.

The last form of nitrogen is residual nitrogen, calculated from measured total non-volatile nitrogen (N_{TOT}) and NO_3^- , NO_2 and $\sum\text{NH}_4^+$ concentration. The residual nitrogen is taken to represent organic nitrogen or

$$N_{residual} = N_{org} = N_{TOT} - \text{NO}_3^- - \text{NO}_2 - \sum\text{NH}_4^+.$$

The relationship of $N_{residual}$ with other nitrogen oxidation states and dissolved organic matter (DOC) is shown in Figure 20. As observed, positive relationship is observed for N_{org} and DOC whereas no relationships is observed between N_{org} and $\sum\text{NH}_4^+$, NO_2 and NO_3^- . This is taken to indicate that $N_{residual}$ originates from dissolved organic matter whereas decomposition of organic matter to NH_4^+ or oxidation to NO_3^- is not a major process.

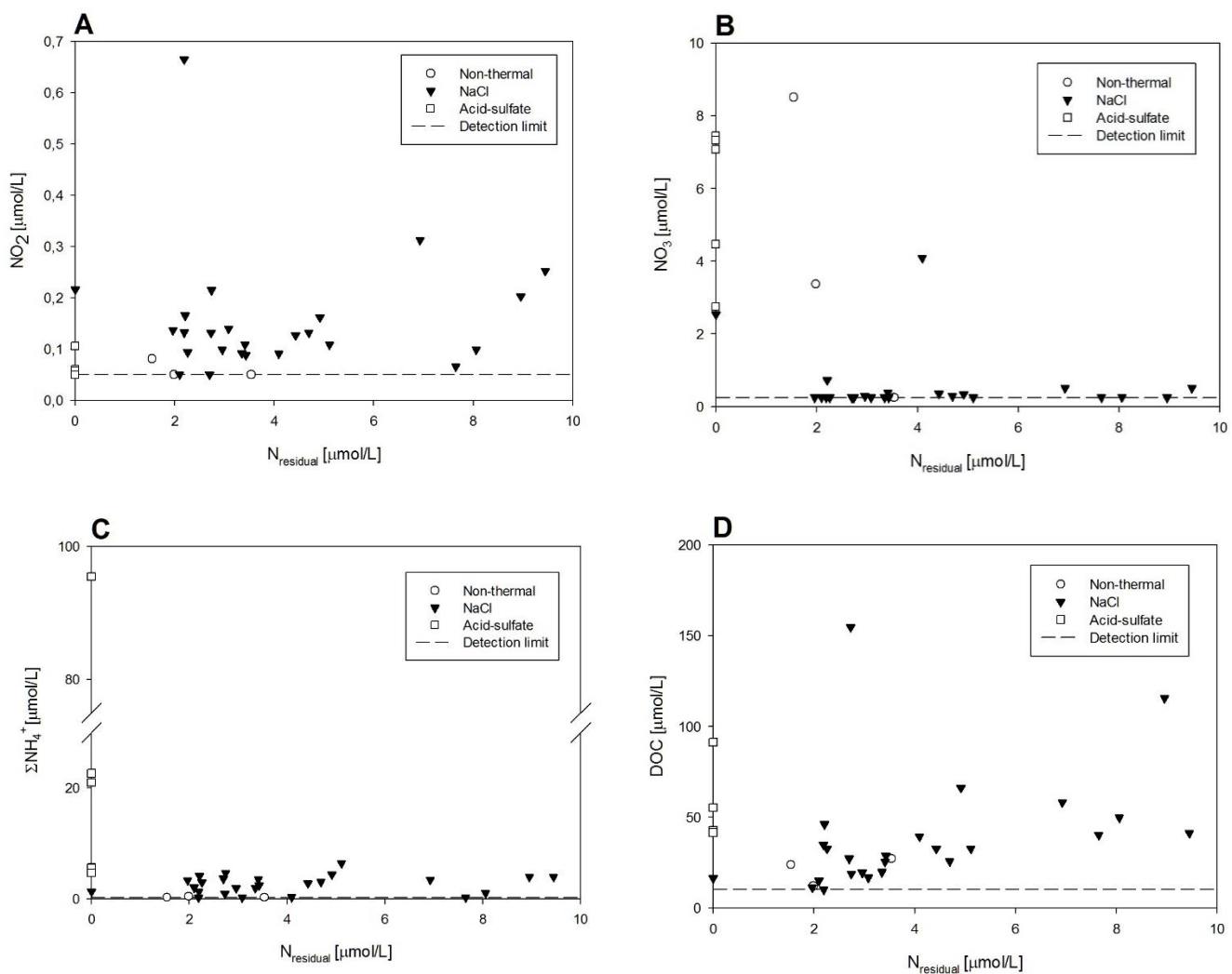


Figure 20 The relationship of $N_{residual}$ with other nitrogen oxidation states and dissolved organic matter (DOC).

4.4 Comparisons to other systems

The average total inorganic nitrogen in precipitation and non-thermal surface waters in Iceland is ~9 µM and 4.4 µM, respectively (Gíslason et al., 1996). In low-temperature waters (<150°C) at Skagafjörður, North-Iceland, ΣNH_4 , NO_3^- and NO_2^- concentrations are <0.005-0.48 µM, <0.001-232 µM and <0.1-6.9 µM, respectively, in waters with temperature of ~0-95°C and pH of ~6.2-10.5 (Stefánsson et al., 2005). River waters in Iceland have somewhat lower concentrations of NO_3^- , NO_2^- and NH_4^+ , or 0.13-0.66 µM, 0.02-0.03 µM and 1.5-3.2 µM respectively (Gíslason et al., 1996) than geothermal waters. Nitrate and NH_3 have been observed to be the most dominant oxidation states in hydrothermal waters with concentrations ranging from <0.01 µM to 232 µM and <0.2 to 6.9 µM, respectively (Stefánsson et al., 2005). Concentrations in non-thermal waters (river waters, peat, soil) in Iceland are also somewhat lower than in thermal waters or <0.15-4.3 µM, <0.04-0.48 µM and <0.2-3.4 µM for NO_3^- , NO_2^- and ΣNH_4 respectively (Stefánsson and Gíslason, 2001). Geothermal waters in Iceland have somewhat lower concentrations of nitrogen species compared to those reported for hydrothermal waters in Yellowstone National Park in the US (Hamilton et al., 2011; Holloway et al., 2011; McCleskey et al., 2010; Shock et al., 2010) but similar to two 80°C hot springs in the US great basin (Hedlund et al., 2011). In high-temperature waters in Iceland (>150°C), N_2 and NH_3 are the dominant species with partial pressures in the reservoir fluids being 0.01-2.99 bar and $1.54\text{-}2.12\cdot10^{-4}$ bar, respectively (Stefánsson and Arnórsson, 2002). The concentrations of inorganic nitrogen, largely in the reduced form of $\Sigma\text{NH}_{4,\text{tot}}$ ranged from a few micromolar to millimolar range in Yellowstone National Park (Holloway et al., 2011) and ranged from around 28-92 µM in the hot springs in the US great basin (Hedlund et al., 2011). The range of concentrations of ΣNH_4 in this research was <0.25-95 µM. In addition to some waters high in ΣNH_4 in the Yellowstone National Park (Holloway et al., 2011), unusually high concentrations of ΣNH_4 up to tens of mM, have also been found associated with geothermal waters elsewhere, for example in Pisciarelly, Italy (Valentino et al., 1999).

As stated before, nitrogen sources in geothermal waters in Iceland are considered to be either meteoric or reactions within geothermal systems. Nitrogen compounds in other volcanic areas have been attributed to magma degassing at depth (Valentino et al., 1999) meteoric waters (Minissale et al., 1997), leaching of rocks by hydrothermal fluids (Allen and Day, 1935; Lowenstern et al., 1999; Minissale et al., 1997; Valentino et al., 1999) and in Yellowstone National Park, nitrogen is considered to originate from thermal decomposition of organic-rich sedimentary rocks (Goff and Janik, 2002) (Goff and Janik, 1993).

5 Summary and conclusions

Nitrogen in low-temperature geothermal waters in Iceland was studied in order to determine its source and reactions within the system. The samples collected were 35, with temperature range of 2-125°C, pH of 2.48-9.72 and total dissolved solids between 801 and 31645 µmol/L. Dissolved N₂ was the most abundant form and therefore the most important species with concentrations of 44-634 µmol/L and counting for up to 100% of nitrogen in the samples. Other nitrogen forms were ammonium, ranging from <0,1-95 µmol/L, nitrite and nitrate concentrations were <0.1-0.66 µmol/L and <0,1-8,51 µmol/L respectively and organic nitrogen concentrations varied from 0-9.44 µmol/L. The oxidation states of nitrogen in geothermal fluids ranged from N(-III) to N(+V).

Various reactions between the oxidation states were studied by calculations of redox potentials for given redox pairs. Activities were then calculated for the overall reactions. For all water types, a redox disequilibrium prevails between various nitrogen containing reactions. Half reactions were balanced against each other in order to study the overall redox reactions and their affinities. Affinities of the reactions ranged from 0,0 kcal/mol e⁻ transferred to 31,7 kcal/mol e⁻ transferred with high affinities for some reactions where H⁺ (H₂O) to H₂ was the electron acceptor and SO₄²⁻ to H₂S was the electron acceptor. Nitrogen reactions seemed to have lower affinities.

Possible nitrogen-redox reactions possible within the system may be summarized into four groups: (1) nitrogen fixation, (2) nitrification, (4) denitrification and (5) organic matter decomposition. Based on the reaction order and affinity calculations, several possible N-containing reactions were observed, including nitrogen fixation and nitrification.

Our study concludes that nitrogen compounds were found to be primarily of two sources. Firstly from the source fluid, originating as precipitation, and secondly upon reactions occurring within the system.

The source of N₂ may be considered to be atmospheric and denitrification, assuming limited deep mantle N₂ source. As observed, most waters are undersaturated with respect to atmospheric N₂, suggesting a possible reduction of N₂ to NH₄⁺. The atmospheric source for N₂ is further supported by the N₂/Ar ratio, which is observed to lie between N₂/Ar ratio of air and N₂/Ar ratio of air saturated water. The source of NO₃ and NO₂ may also be the source water, i.e. it does not produce upon reactions within the system. The origin of N_{residual} is considered to be from dissolved organic matter.

References

- Allen, E.T., Day, A.L. (1935). Hot springs of the Yellowstone National Park.
- Árnason, B. (1976). Groundwater systems in Iceland traced by deuterium. *Vísindafélag Íslendinga* 42, 236.
- Árnason, B. (1977). Hydrothermal systems in Iceland traced by deuterium. *Geothermics* 5, 125-151.
- Arnórsson, S. (1986). Chemistry of gases associated with geothermal activity and volcanism in Iceland: a review. *J. Geophys. Res.* 91, 12,261-212,268.
- Arnórsson, S. (1995). Geothermal systems in Iceland: Structure and conceptual models-II. Low-temperature areas. *Geothermics* 24, 603-629.
- Arnórsson, S., Andrésdóttir, A. (1995). Processes controlling the distribution of boron and chlorine in natural waters in Iceland. *Geochimica et Cosmochimica Acta* 59, 4125-4146.
- Arnórsson, S., Sigurðsson, S., Svavarsson, H. (1982). The chemistry of geothermal waters in Iceland. I. Calculation of aqueous speciation from 0° to 370°C. *Geochimica et Cosmochimica Acta* 46, 1513-1532.
- Arnórsson, S., Stefánsson, A., Bjarnason, J.Ö. (2007). Fluid-fluid interaction in geothermal systems. *Reviews in Mineralogy and Geochemistry* 65.
- Clor, L.E., Fischer, T.P., Hilton, D.R., Sharp, Z.D., Hartono, U. (2005). Volatile and N isotope chemistry of the Molucca Sea collision zone: tracing source components along the Sangihe Arc, Indonesia. *Geochemistry, Geophysics, Geosystems* 6, 20.
- Fischer, T.P., Burnard, P., Marty, B., Hilton, D.R., E., F., F., P., D., S.Z., Mangasini, F. (2009). Upper-mantle volatile chemistry at Oldoinyo Lengai volcano and the origin of carbonates. *Nature* 459, 77-80.
- Fischer, T.P., Hilton, D.R., Zimmer, M.M., Shaw, A.M., Sharp, Z.D., Walker, J.A. (2002). Subduction and recycling of nitrogen along the Central American margin. *Science* 297, 1154-1157.
- Fournier, R.O. (1989). Geochemistry and dynamics of the Yellowstone National Park hydrothermal system. *Annual Review of Earth and Planetary Sciences* 17, 13.
- Gíslason, S.R., Arnórsson, S., Ármannsson, H. (1996). Chemical weathering of basalt in Southwest Iceland; effects of runoff, age of rocks and vegetative/glacial cover. *American Journal of Science* 296, 837-907.
- Goff, F., Janik, C.J. (1993). Gas geochemistry and guide for geothermal features in the Clear Lake region, California. *Active geothermal systems and gold-mercury deposits in the Sonoma-Clear Lake volcanic fields, California: Society of Economic Geologists Guidebook Series* 16, 207-261.
- Goff, F., Janik, C.J. (2002). Gas geochemistry of the Valles caldera region, New Mexico and comparisons with gases at Yellowstone, Long Valley and other geothermal systems. *Journal of volcanology and geothermal research* 116, 299-323.
- Hamilton, T.L., Lange, R.K., Boyd, E.S., Peters, J.W. (2011). Biological nitrogen fixation in acidic high-temperature geothermal springs in Yellowstone National Park, Wyoming. *Environmental microbiology* 13, 2204-2215.
- Hedlund, B.P., McDonald, A., Lam, J., Dodsworth, J., Brown, J., Hungate, B. (2011). Potential role of *Thermus thermophilus* and *T. oshimai* in high rates of nitrous oxide (N₂O) production in < 80°C hot springs in the US Great Basin. *Geobiology* 9, 471-480.

- Heitz, E., Flemming, H., Sand, W., 1996. Microbially influenced corrosion of materials: scientific and engineering aspects. Springer-Verlag.
- Holloway, J.M., Nordstrom, D.K., Böhlke, J.K., McCleskey, R.B., Ball, J.W. (2011). Ammonium in thermal waters of Yellowstone National Park: processes affecting speciation and isotope fractionation. *Geochimica et Cosmochimica Acta* 75, 4611-4636.
- Linberg, R.D., Runnels, D. (1984). Ground water redox reactions: an analysis of equilibrium state applied to Eh measurements and geochemical modeling. *Science* 225, 925-927.
- Lowenstern, J.B., Bergfeld, D., Evans, W.C., Hurwitz, S. (2012). Generation and evolution of hydrothermal fluids at Yellowstone: insights from the Heart Lake Geyser Basin. *Geochemistry, Geophysics, Geosystems* 13.
- Lowenstern, J.B., Janik, C.J., Fahlquist, L., Johnson, L.S., 1999. Compilation of gas geochemistry and isotopic analyses from The Geysers geothermal field: 1978-1991, Geothermal Resources Council Transactions, pp. 383-390.
- McCleskey, R.B., Nordstrom, D.K., Susong, D.D., Ball, J.W., Holloway, J.M. (2010). Source and fate of inorganic solutes in the Gibbon River, Yellowstone National Park, Wyoming, USA: I. Low-flow discharge and major solute chemistry. *Journal of Volcanology and Geothermal Research* 193, 189-202.
- Minissale, A., Magro, G., Vaselli, O., Verrucchi, C., Perticone, I. (1997). Geochemistry of water and gas discharges from the Mt. Amiata silicic complex and surrounding areas (central Italy). *Journal of Volcanology and Geothermal research* 79, 223-251.
- Óskarsson, F., Inguaggiato, S., Friðriksson, P., Caliro, S. (2015). Gas Isotope Characterisation of the Reykjanes Geothermal Field, Iceland. *Proceedings World Geothermal Congress, Melbourne*.
- Parkhurst, D.L., Appelo, C.A.J., 1999. User's guide to PHREEQC (version 2) - A computer program for speciation, batch-reaction, one-dimensional transport, and inverse geochemical calculations., USGS Water Resources Investigations Report 99-4259, p. 312.
- Sand, W. (2003). Microbial life in geothermal waters. *Geothermics* 32, 655-667.
- Sano, Y., Takahata, N., Nishio, Y., Marty, B. (1998). Nitrogen recycling in subduction zone. *Geophys. Res. Lett.* 25, 2289-2292.
- Sano, Y., Takahata, N., Noishio, Y., Fischer, T.P., Williams, S.N. (2001). Volcanic flux of nitrogen from the Earth. *Chem. Geol.* 171, 363-371.
- Shock, E.L., Holland, M., Amend, J.P., Osburn, G.R., Fischer, T.P. (2010). Quantifying inorganic sources of geochemical energy in hydrothermal ecosystems, Yellowstone National Park, USA. *Geochimica et Cosmochimica Acta* 74, 4005-4043.
- Stefánsson, A., Arnórsson, S. (2002). Gas pressures and redox reactions in geothermal fluids in Iceland. *Chemical Geology* 190, 251-271.
- Stefánsson, A., Arnórsson, S., Sveinbjörnsdóttir, Á.E. (2005). Redox reactions and potentials in natural waters at disequilibrium. *Chemical Geology* 221, 289-311.
- Stefánsson, A., Gíslason, S.R. (2001). Chemical weathering of basalts, Southwest Iceland: effect of rock crystallinity and secondary minerals on chemical fluxes to the ocean. *American Journal of Science* 301, 513-556.
- Stumm, W., Morgan, J., 2012. Aquatic chemistry: chemical equilibria and rates in natural waters. John Wiley & Sons.
- Valentino, G.M., Cortecchi, G., Franco, E., Stanzione, D. (1999). Chemical and isotopic compositions of minerals and waters from the Campi Flegrei volcanic system, Naples, Italy. *Journal of Volcanology and Geothermal Research* 91, 329-344.

Appendix A

Redox potentials (pe)

#	t°C	pH _T	pe								
			H ₂ O/O ₂	H ₂ /H ⁺	H ₂ S/SO ₄	NH ₄ /NO ₃	NH ₄ /NO ₂	NH ₄ /N ₂	N ₂ /NO ₂	N ₂ /NO ₃	NO ₂ /NO ₃
14-RSA-1	69	7,27	9,93	-5,36	-4,08	4,01		-3,71		8,64	
14-RSA-2	4	9,26								10,09	
14-RSA-3	60	8,74	8,47	-6,50	-5,80		1,99	-5,56	9,54		
14-RSA-4	100	8,34			-5,39	1,78	1,26				3,34
14-RSA-5	2	9,32				4,53					
14-RSA-6	96	8,26	8,12		-5,29	1,97	1,52	-5,12	8,16	6,22	3,32
14-RSA-7	97	8,13	7,75		-5,15	2,08	1,62	-5,12	8,36	6,40	3,46
14-RSA-8	38	7,27	12,06	-4,71		5,38		-3,24		10,55	
14-RSA-9	69	7,36	10,24					-5,82			
14-RSA-10	7	7,70									
14-RSA-11	86	7,41	9,12		-4,27	3,18	2,74	-4,29	9,77	7,67	4,52
14-RSA-12	99	8,16	7,66	-5,40	-5,20	1,99	1,48	-5,16	8,12	6,27	3,50
14-RSA-13	100	8,21			-5,26	1,89	1,42		7,31		3,32
14-RSA-14	101	8,15	7,68		-5,19	1,96	1,48	-5,09	8,05	6,19	3,41
14-RSA-15	87	7,93	8,50	-5,50	-4,84			-4,73			
14-RSA-16	78	8,82	8,03		-5,66			-5,67			
14-RSA-17	68	8,95	8,42	-6,85	-5,89	1,98		-5,72		6,61	
14-RSA-18	27	9,72	10,29		-6,54			-6,29			
14-RSA-19	95	8,70	7,31		-5,76	1,46	0,95	-5,73	7,64	5,77	2,96
14-RSA-20	75	8,49	8,52		-5,42	2,29		-5,41		6,91	
14-RSA-21	72	8,85	8,35	-5,96	-5,86	2,08	1,66	-5,25	8,58	6,48	3,34
14-RSA-22	71	9,23	8,16		-6,32	1,67	1,36	-5,62	8,35	6,05	2,59
14-RSA-23	68	9,21	8,16		-6,20	1,71	1,23	-5,96	8,42	6,32	3,17
14-RSA-24	63	9,69	7,97	-7,62		1,47	0,86	-6,34	8,07	6,16	3,31
14-RSA-25	125	8,22	6,47	-5,61	-5,34	1,27	0,80	-5,20	6,80	5,15	2,68
14-RSA-26	89	8,92	7,36	-6,82	-5,92		0,97	-5,63	7,57		
14-RSA-28	105	7,80	7,60		-4,70		1,79	-4,81	8,38		
14-RSA-29	77	8,86	7,72	-6,42	-5,89	1,77		-5,62		6,20	
14-RSA-30	98	3,01	13,03			8,34		0,97		12,76	
14-RSA-31	56	3,19	15,09			9,63		1,59		14,46	
14-RSA-32	85	3,26	13,46			8,56		1,19		12,99	
14-RSA-33	36	4,35				8,90					
14-RSA-34	89	2,94				8,72	8,44				9,53
14-RSA-37	76	2,48				9,85					

Appendix B

Calculated logQ values for the reactions of interest

#	t°C	pHT	logQ																						
			100-1	100-20	100-21	100-22	100-23	100-24	100-25	200-1	200-20	200-21	200-22	200-23	200-24	200-25	500-1	500-2	500-20	500-21	500-22	500-23	500-24	500-25	
14-RSA-1	69	7,27	9,3	-2,2		3,1		-7,6		-9,3	-39,4	-26,7	-24,7		-54,0		0,1	37,2	8,1		12,6		-44,6		
14-RSA-2	4	9,26																							
14-RSA-3	60	8,74	11,1		-5,8	3,1	-14,6			-11,1		-38,9	-30,1	-47,7				-1,4	42,8		-27,2	8,1	-62,5		
14-RSA-4	100	8,34																		10,2	-26,9			16,4	
14-RSA-5	2	9,32																							
14-RSA-6	96	8,26		-8,2	-10,5	-1,1	-19,8	-15,2	2,3									5,4		9,2	-25,8	11,7	-63,2	-50,4	14,6
14-RSA-7	97	8,13		-4,4	-7,7	0,9	-16,4	-9,8	3,3									1,7		9,0	-26,0	8,5	-60,5	-47,0	14,9
14-RSA-8	38	7,27	10,5	-3,1		1,9		-8,0		-10,5	-45,2	-31,9	-29,7		-60,8										
14-RSA-9	69	7,36																							
14-RSA-10	7	7,70																							
14-RSA-11	86	7,41		-5,0	-8,1	0,2	-16,4	-10,2	3,1									1,6		7,6	-27,6	5,6	-60,8	-47,5	14,0
14-RSA-12	99	8,16	10,2	-4,8	-8,2	0,7	-17,2	-10,3	3,5	-10,2	-45,4	-38,7	-29,8	-47,7	-61,1	-6,7	2,0	42,7	9,2	-26,8	9,1	-62,8	-47,2	15,9	
14-RSA-13	100	8,21																		9,2	-26,3			15,2	
14-RSA-14	101	8,15		-5,4	-8,6	0,7	-17,8	-11,4	3,2									2,7	9,3	-26,1	10,7	-62,9	-48,3	15,5	
14-RSA-15	87	7,93	9,6				0,9			-9,6		-30,1	-27,8					1,8	40,1			9,0			
14-RSA-16	78	8,82					0,3											1,2			4,7				
14-RSA-17	68	8,95	9,4	-6,3		0,2		-12,7		-9,4	-43,7	-30,6	-27,9		-59,4		2,3	39,7	10,9		7,6		-56,9		
14-RSA-18	27	9,72					-2,1											4,1			3,9				
14-RSA-19	95	8,70		-5,7	-8,9	0,2	-18,1	-11,6	3,2									2,4		10,1	-28,6	8,1	-65,3	-52,0	15,4
14-RSA-20	75	8,49		-5,6		-0,2		-11,1									1,8		9,7		4,6		-52,3		
14-RSA-21	72	8,85	10,8	-5,5	-8,4	2,5	-19,3	-13,5	2,9	-10,8	-48,9	-40,9	-30,0	-51,8	-67,7	-7,9	2,9	46,2	10,8	-25,0	18,6	-68,5	-57,4	14,4	
14-RSA-22	71	9,23		-7,0	-8,9	1,8	-19,5	-15,8	1,8								4,6		12,6	-21,7	20,9	-64,3	-58,8	12,0	
14-RSA-23	68	9,21		-6,3	-9,4	0,5	-19,2	-13,0	3,1								2,5		11,3	-30,1	9,3	-69,5	-58,0	14,9	
14-RSA-24	63	9,69	9,4	-5,9	-9,9	0,6	-20,4	-12,4	4,0	-9,4	-43,6	-38,2	-27,7	-48,6	-59,5	-5,4								27,6	
14-RSA-25	125	8,22	9,4	-4,5	-7,7	2,2	-17,7	-11,1	3,3	-9,4	-42,2	-36,0	-26,1	-45,9	-58,3	-6,2	2,1	39,8	10,1	-24,5	15,2	-64,2	-50,3	15,2	
14-RSA-26	89	8,92	9,0		-8,5	2,0	-19,0			-9,0		-35,6	-25,1	-46,1				1,9	38,1		-28,3	13,6	-70,3		
14-RSA-28	105	7,80		-6,7	1,9	-15,2												-0,4		-28,0	6,2	-62,2			
14-RSA-29	77	8,86	10,5	-3,8		2,7		-10,3		-10,5	-45,7	-31,9	-28,8		-62,7		0,3	42,2	10,9		11,4		-57,7		
14-RSA-30	98	3,01				3,2		5,5		0,9															
14-RSA-31	56	3,19				3,6		7,3		-0,2															
14-RSA-32	85	3,26				3,5		7,3		-0,3															
14-RSA-33	36	4,35																							
14-RSA-34	89	2,94																						15,2	
14-RSA-37	76	2,48																							

Appendix B *continued*

#	logQ																						
	2100-2	2100-5	2100-21	2100-22	2100-23	2100-24	2100-25	2200-1	2200-3	2200-5	2200-21	2200-22	2200-23	2200-24	2200-25	2300-1	2300-2	2300-5	2300-21	2300-22	2300-23	2300-24	2300-25
14-RSA-1	39,4	2,2		19,1		-19,1										-3,1	24,7	-12,6	-19,1			-38,3	
14-RSA-2																							
14-RSA-3																							
14-RSA-4		2,6	-19,0					19,0		5,8	38,9	27,2		8,8	-8,8			-3,1	30,1	-8,1		-8,8	-17,7
14-RSA-5												26,9	19,0					19,0					
14-RSA-6		2,8	-17,4	20,0	-54,8	-20,0	17,4	10,5		25,8	17,4	9,4	-9,4	6,8	17,4	1,1		-11,7	-20,0	-9,4	-18,7	-40,0	8,1
14-RSA-7		2,8	-17,7	16,9	-52,2	-16,9	17,7	7,7		26,0	17,7	8,6	-8,6	9,4	17,7	-0,9		-8,5	-16,9	-8,6	-17,3	-33,7	9,0
14-RSA-8	45,2			16,9		-16,9										-1,9	29,7		-16,9				-33,8
14-RSA-9																							
14-RSA-10																							
14-RSA-11		3,4	-17,4	15,8	-50,6	-15,8	17,4	8,1		27,6	17,4	8,3	-8,3	10,0	17,4	-0,2		-5,6	-15,8	-8,3	-16,6	-31,6	9,1
14-RSA-12	45,4	2,7	-18,7	17,3	-54,6	-17,3	18,7	8,2	38,7	26,8	18,7	9,0	-9,0	10,4	18,7	-0,7	29,8	-9,1	-17,3	-9,0	-18,0	-34,6	9,7
14-RSA-13		2,8	-17,9					17,9			26,3	17,9					17,9						
14-RSA-14		2,7	-18,1	18,7	-55,0	-18,7	18,1	8,6		26,1	18,1	9,2	-9,2	8,6	18,1	-0,7		-10,7	-18,7	-9,2	-18,4	-37,4	8,9
14-RSA-15																-0,9	27,8	-9,0					
14-RSA-16																-0,3		-4,7					
14-RSA-17	43,7	3,9		19,4		-19,4										-0,2	27,9	-7,6	-19,4			-38,8	
14-RSA-18																2,1		-3,9					
14-RSA-19		3,3	-18,7	18,0	-55,4	-18,0	18,7	8,9		28,6	18,7	9,2	-9,2	9,8	18,7	-0,2		-8,1	-18,0	-9,2	-18,4	-36,1	9,5
14-RSA-20		3,8		16,1		-16,1										0,2		-4,6	-16,1			-32,3	
14-RSA-21	48,9	2,6	-17,1	26,5	-60,7	-26,5	17,1	8,4	40,9	25,0	17,1	10,9	-10,9	1,4	17,1	-2,5	30,0	-18,6	-26,5	-10,9	-21,8	-53,1	6,2
14-RSA-22		2,4	-14,4	28,2	-57,0	-28,2	14,4	8,9		21,7	14,4	10,6	-10,6	-3,1	14,4	-1,8		-20,9	-28,2	-10,6	-21,3	-56,3	3,8
14-RSA-23		3,8	-18,7	20,7	-58,1	-20,7	18,7	9,4		30,1	18,7	9,8	-9,8	7,9	18,7	-0,5		-9,3	-20,7	-9,8	-19,7	-41,3	8,9
14-RSA-24	43,6		-21,8	20,1	-63,7	-20,1	21,8	9,9	38,2		21,8	10,5	-10,5	12,3	21,8	-0,6	27,7		-20,1	-10,5	-20,9	-40,1	11,4
14-RSA-25	42,2	2,3	-17,5	22,2	-57,2	-22,2	17,5	7,7	36,0	24,5	17,5	9,9	-9,9	5,2	17,5	-2,2	26,1	-15,2	-22,2	-9,9	-19,9	-44,4	7,6
14-RSA-26									8,5	35,6	28,3		10,5	-10,5		-2,0	25,1	-13,6		-10,5	-21,0		
14-RSA-28								6,7		28,0		8,5	-8,5			-1,9		-6,2		-8,5	-17,1		
14-RSA-29	45,7	3,6		22,1		-22,1										-2,7	28,8	-11,4	-22,1			-44,2	
14-RSA-30				12,4		-12,4										-5,5		-12,4			-24,8		
14-RSA-31				18,6		-18,6										-7,3		-18,6			-37,3		
14-RSA-32				18,6		-18,6										-7,3		-18,6			-37,3		
14-RSA-33																							
14-RSA-34				-13,3				13,3								13,3							
14-RSA-37																							

Appendix B *continued*

#	logQ																									
	2400-1	2400-2	2400-5	2400-21	2400-22	2400-23	2500-24	2400-25	2500-1	2500-2	2500-5	2500-21	2500-22	2500-23	2500-24	2500-25	2600-1	2600-2	2600-5	2600-21	2600-22	2600-23	2600-24	2600-25		
14-RSA-1									7,6	54,0	30,1	19,1		38,3												
14-RSA-2																										
14-RSA-3	14,6	47,7	62,5			8,8	17,7			48,1																
14-RSA-4																					-16,4	-19,0	-19,0			
14-RSA-5																										
14-RSA-6	19,8		63,2	54,8	9,4	18,7	53,5	26,8	15,2		33,9	20,0	-6,8	40,0	-53,5	26,8	-2,3		-14,6	-17,4	-17,4	-8,1	-26,8	-26,8		
14-RSA-7	16,4		60,5	52,2	8,6	17,3	52,6	26,3	9,8		30,8	16,9	-9,4	33,7	-52,6	26,3	-3,3		-14,9	-17,7	-17,7	-9,0	-26,3	-26,3		
14-RSA-8									8,0	60,8		16,9		33,8												
14-RSA-9																										
14-RSA-10																										
14-RSA-11	16,4		60,8	50,6	8,3	16,6	51,5	25,7	10,2		32,7	15,8	-10,0	31,6	-51,5	25,7	-3,1		-14,0	-17,4	-17,4	-9,1	-25,7	-25,7		
14-RSA-12	17,2	47,7	62,8	54,6	9,0	18,0	55,3	27,6	10,3	61,1	30,9	17,3	-10,4	34,6	-55,3	27,6	-3,5	6,7	-15,9	-18,7	-18,7	-9,7	-27,6	-27,6		
14-RSA-13																				-15,2	-17,9	-17,9				
14-RSA-14	17,8		62,9	55,0	9,2	18,4	54,7	27,3	11,4		32,0	18,7	-8,6	37,4	-54,7	27,3	-3,2		-15,5	-18,1	-18,1	-8,9	-27,3	-27,3		
14-RSA-15										46,0																
14-RSA-16																										
14-RSA-17											12,7	59,4	39,0	19,4		38,8										
14-RSA-18																										
14-RSA-19	18,1		65,3	55,4	9,2	18,4	55,7	27,9	11,6		34,6	18,0	-9,8	36,1	-55,7	27,9	-3,2		-15,4	-18,7	-18,7	-9,5	-27,9	-27,9		
14-RSA-20										11,1		35,3	16,1		32,3											
14-RSA-21	19,3	51,8	68,5	60,7	10,9	21,8	55,9	28,0	13,5	67,7	39,7	26,5	-1,4	53,1	-55,9	28,0	-2,9	7,9	-14,4	-17,1	-17,1	-6,2	-28,0	-28,0		
14-RSA-22	19,5		64,3	57,0	10,6	21,3	50,1	25,0	15,8		40,4	28,2	3,1	56,3	-50,1	25,0	-1,8		-12,0	-14,4	-14,4	-3,8	-25,0	-25,0		
14-RSA-23	19,2		69,5	58,1	9,8	19,7	57,1	28,6	13,0		39,6	20,7	-7,9	41,3	-57,1	28,6	-3,1		-14,9	-18,7	-18,7	-8,9	-28,6	-28,6		
14-RSA-24	20,4	48,6		63,7	10,5	20,9	64,6	32,3	12,4	59,5		20,1	-12,3	40,1	-64,6	32,3	-4,0	5,4		-21,8	-21,8	-11,4	-32,3	-32,3		
14-RSA-25	17,7	45,9	64,2	57,2	9,9	19,9	54,8	27,4	11,1	58,3	33,9	22,2	-5,2	44,4	-54,8	27,4	-3,3	6,2	-15,2	-17,5	-17,5	-7,6	-27,4	-27,4		
14-RSA-26	19,0	46,1	70,3		10,5	21,0				44,4																
14-RSA-27	15,2		62,2			8,5	17,1																			
14-RSA-28											10,3	62,7	40,0	22,1		44,2			13,8							
14-RSA-29											-0,9		12,4		24,8											
14-RSA-30											0,2		18,6		37,3											
14-RSA-31											0,3		18,6		37,3											
14-RSA-32																										
14-RSA-33																										
14-RSA-34																										
14-RSA-35																										
14-RSA-36																										
14-RSA-37																										

Appendix C

Calculated logK values for the reactions of interest

#	t°C	pHT	logK																					
			100-1	100-20	100-21	100-22	100-23	100-24	100-25	200-1	200-20	200-21	200-22	200-23	200-24	200-25	500-1	500-2	500-20	500-21	500-22	500-23	500-24	500-25
14-RSA-1	69	7.27	39.9	45.2	32.1	85.0	-20.7	5.4	13.1	-39.9	-114.3	-87.5	-34.6	-140.4	-194.0	-26.8	-112.1	47.4	-66.9	-207.8	3.6	-419.2	-538.9	-59.8
14-RSA-2	4	9.26	49.7	57.2	40.7	105.7	-24.3	8.7	16.5	-49.7	-141.7	-108.5	-43.5	-173.5	-239.9	-33.2	-142.4	56.5	-85.2	-264.3	-4.4	-524.3	-677.2	-76.4
14-RSA-3	60	8.74	41.0	46.6	33.1	87.2	-21.0	5.9	13.4	-41.0	-117.3	-89.8	-35.7	-143.9	-199.0	-27.5	-115.5	48.4	-69.0	-214.1	2.4	-430.6	-554.1	-61.7
14-RSA-4	100	8.34	36.2	40.5	28.7	77.4	-20.0	3.5	11.8	-36.2	-104.2	-79.8	-31.1	-128.5	-177.3	-24.4	-100.5	44.2	-60.0	-186.6	8.2	-381.5	-488.5	-53.5
14-RSA-5	2	9.32	50.1	57.7	41.0	106.5	-24.4	8.8	16.6	-50.1	-142.7	-109.3	-43.8	-174.8	-241.7	-33.5	-143.5	56.9	-85.9	-266.5	-4.5	-528.4	-682.5	-77.0
14-RSA-6	96	8.26	36.6	41.0	29.1	78.3	-20.1	3.7	11.9	-36.6	-105.4	-80.7	-31.5	-129.9	-179.3	-24.7	-101.9	44.6	-60.8	-189.1	7.6	-385.9	-494.4	-54.2
14-RSA-7	97	8.13	36.5	40.9	29.0	78.1	-20.0	3.7	11.9	-36.5	-105.1	-80.5	-31.4	-129.5	-178.8	-24.6	-101.5	44.5	-60.6	-188.5	7.8	-384.8	-492.9	-54.1
14-RSA-8	38	7.27	44.1	50.4	35.9	93.7	-22.0	7.1	14.5	-44.1	-126.0	-96.4	-38.6	-154.3	-213.4	-29.6	-125.2	51.2	-74.8	-232.0	-0.6	-463.4	-597.5	-67.0
14-RSA-9	69	7.36	39.9	45.2	32.1	84.9	-20.7	5.4	13.1	-39.9	-114.3	-87.5	-34.6	-140.3	-193.9	-26.8	-112.0	47.4	-66.9	-207.7	3.7	-419.1	-538.7	-59.8
14-RSA-10	7	7.70	49.3	56.7	40.3	104.7	-24.0	8.6	16.3	-49.3	-140.4	-107.4	-43.1	-171.8	-237.7	-32.9	-141.0	56.1	-84.3	-261.6	-4.1	-519.1	-670.4	-75.6
14-RSA-11	86	7.41	37.8	42.5	30.2	80.7	-20.3	4.4	12.3	-37.8	-108.6	-83.1	-32.6	-133.6	-184.5	-25.5	-105.5	45.6	-63.0	-195.8	6.1	-397.8	-510.3	-56.3
14-RSA-12	99	8.16	36.3	40.6	28.8	77.6	-20.0	3.6	11.8	-36.3	-104.5	-80.0	-31.2	-128.8	-177.8	-24.5	-100.8	44.3	-60.2	-187.3	8.0	-382.6	-489.9	-53.7
14-RSA-13	100	8.21	36.1	40.4	28.7	77.4	-20.0	3.5	11.7	-36.1	-104.1	-79.7	-31.1	-128.4	-177.2	-24.4	-100.4	44.2	-60.0	-186.5	8.2	-381.3	-488.2	-53.4
14-RSA-14	101	8.15	36.1	40.4	28.6	77.3	-20.0	3.5	11.7	-36.1	-104.0	-79.6	-31.0	-128.2	-176.9	-24.4	-100.2	44.1	-59.9	-186.2	8.3	-380.6	-487.3	-53.3
14-RSA-15	87	7.93	37.6	42.3	30.0	80.3	-20.2	4.3	12.3	-37.6	-108.0	-82.7	-32.5	-133.0	-183.6	-25.3	-104.9	45.4	-62.7	-194.7	6.4	-395.8	-507.6	-55.9
14-RSA-16	78	8.82	38.7	43.7	31.0	82.5	-20.5	4.8	12.6	-38.7	-111.1	-85.0	-33.5	-136.5	-188.6	-26.0	-108.4	46.4	-64.7	-201.0	5.0	-407.0	-522.6	-57.8
14-RSA-17	68	8.95	39.9	45.2	32.1	85.0	-20.7	5.4	13.1	-39.9	-114.3	-87.5	-34.7	-140.4	-194.0	-26.8	-112.1	47.4	-66.9	-207.8	3.6	-419.3	-539.1	-59.9
14-RSA-18	27	9.72	45.8	52.6	37.4	97.4	-22.6	7.7	15.1	-45.8	-130.8	-100.1	-40.1	-160.1	-221.5	-30.7	-130.5	52.8	-78.0	-241.9	-2.0	-481.9	-621.8	-70.0
14-RSA-19	95	8.70	36.7	41.1	29.2	78.5	-20.1	3.8	11.9	-36.7	-105.6	-80.9	-31.6	-130.2	-179.7	-24.8	-102.2	44.6	-61.0	-189.7	7.5	-386.8	-495.6	-54.4
14-RSA-20	75	8.49	39.1	44.2	31.4	83.4	-20.6	5.0	12.8	-39.1	-112.3	-85.9	-33.9	-137.9	-190.6	-26.3	-109.7	46.7	-65.5	-203.5	4.5	-411.5	-528.6	-58.6
14-RSA-21	72	8.85	39.5	44.6	31.7	84.1	-20.6	5.2	12.9	-39.5	-113.2	-86.6	-34.2	-139.0	-192.1	-26.5	-110.8	47.0	-66.1	-205.4	4.1	-414.9	-533.2	-59.1
14-RSA-22	71	9.23	39.6	44.8	31.9	84.4	-20.7	5.2	13.0	-39.6	-113.6	-86.9	-34.4	-139.5	-192.8	-26.6	-111.2	47.2	-66.4	-206.3	3.9	-416.5	-535.2	-59.4
14-RSA-23	68	9.21	40.0	45.3	32.2	85.2	-20.8	5.4	13.1	-40.0	-114.6	-87.7	-34.8	-140.7	-194.5	-26.9	-112.4	47.5	-67.1	-208.4	3.5	-420.4	-540.5	-60.0
14-RSA-24	63	9.69	40.6	46.1	32.8	86.5	-20.9	5.7	13.3	-40.6	-116.3	-89.0	-35.3	-142.7	-197.3	-27.3	-114.4	48.1	-68.3	-212.0	2.8	-426.8	-549.0	-61.1
14-RSA-25	125	8.22	33.6	37.2	26.3	72.2	-19.6	2.1	10.8	-33.6	-97.2	-74.4	-28.5	-120.4	-165.9	-22.7	-92.4	42.0	-55.2	-171.9	11.8	-355.6	-453.6	-49.0
14-RSA-26	89	8.92	37.4	42.1	29.9	80.0	-20.2	4.2	12.2	-37.4	-107.6	-82.4	-32.3	-132.5	-182.9	-25.2	-104.4	45.3	-62.4	-193.8	6.6	-394.1	-505.4	-55.6
14-RSA-28	105	7.80	35.6	39.8	28.2	76.4	-19.9	3.2	11.6	-35.6	-102.8	-78.7	-30.6	-126.8	-175.0	-24.1	-98.9	43.7	-59.1	-183.7	8.9	-376.2	-481.4	-52.6
14-RSA-29	77	8.86	38.8	43.8	31.1	82.7	-20.5	4.8	12.7	-38.8	-111.3	-85.2	-33.6	-136.8	-189.0	-26.1	-108.6	46.4	-64.9	-201.5	4.9	-407.8	-523.7	-58.0
14-RSA-30	98	3.01	36.4	40.8	28.9	77.9	-20.0	3.6	11.8	-36.4	-104.8	-80.2	-31.3	-129.2	-178.3	-24.6	-101.2	44.4	-60.4	-187.9	7.9	-383.7	-491.4	-53.9
14-RSA-31	56	3.19	41.5	47.2	33.6	88.4	-21.2	6.1	13.6	-41.5	-118.8	-90.9	-36.2	-145.7	-201.5	-27.9	-117.2	48.9	-70.0	-217.2	1.9	-436.2	-561.5	-62.7
14-RSA-32	85	3.26	37.9	42.6	30.3	80.9	-20.3	4.4	12.3	-37.9	-108.8	-83.3	-32.7	-133.9	-184.9	-25.5	-105.8	45.6	-63.2	-196.3	6.0	-398.6	-511.4	-56.4
14-RSA-33	36	4.35	44.5	50.9	36.2	94.5	-22.1	7.2	14.7	-44.5	-126.9	-97.1	-38.9	-155.4	-215.0	-29.8	-126.3	51.5	-75.4	-234.0	-0.9	-467.1	-602.3	-67.6
14-RSA-34	89	2.94	37.4	42.0	29.9	79.9	-20.2	4.2	12.2	-37.4	-107.6	-82.4	-32.3	-132.4	-182.9	-25.2	-104.4	45.2	-62.3	-193.7	6.6	-394.0	-505.2	-55.6
14-RSA-37	76	2.48	39.0	44.0	31.3	83.1	-20.5	4.9	12.7	-39.0	-111.9	-85.6	-33.8	-137.5	-190.0	-26.2	-109.3	46.6	-65.3	-202.7	4.7	-410.1	-526.7	-58.3

Appendix C *continued*

#	logK																							
	2100-1	2100-2	2100-5	2100-21	2100-22	2100-23	2100-24	2100-25	2200-1	2200-3	2200-5	2200-21	2200-22	2200-23	2200-24	2200-25	2300-1	2300-2	2300-5	2300-21	2300-22	2300-23	2300-24	2300-25
14-RSA-1	-45.2	114.3	66.9	-7.1	204.4	-218.5	-204.4	7.1	-32.1	87.5	207.8	7.1	52.9	-52.9	-144.5	7.1	-85.0	34.6	-3.6	-204.4	-52.9	-105.7	-408.7	-45.8
14-RSA-2	-57.2	141.7	85.2	-8.8	251.2	-268.7	-251.2	8.8	-40.7	108.5	264.3	8.8	65.0	-65.0	-177.5	8.8	-105.7	43.5	4.4	-251.2	-65.0	-130.0	-502.4	-56.2
14-RSA-3	-46.6	117.3	69.0	-7.2	209.3	-223.7	-209.3	7.2	-33.1	89.8	214.1	7.2	54.1	-54.1	-148.0	7.2	-87.2	35.7	-2.4	-209.3	-54.1	-108.3	-418.6	-46.9
14-RSA-4	-40.5	104.2	60.0	-6.5	188.3	-201.4	-188.3	6.5	-28.7	79.8	186.6	6.5	48.7	-48.7	-133.0	6.5	-77.4	31.1	-8.2	-188.3	-48.7	-97.4	-376.6	-42.2
14-RSA-5	-57.7	142.7	85.9	-8.8	253.1	-270.8	-253.1	8.8	-41.0	109.3	266.5	8.8	65.5	-65.5	-178.8	8.8	-106.5	43.8	4.5	-253.1	-65.5	-131.0	-506.2	-56.6
14-RSA-6	-41.0	105.4	60.8	-6.6	190.2	-203.4	-190.2	6.6	-29.1	80.7	189.1	6.6	49.2	-49.2	-134.4	6.6	-78.3	31.5	-7.6	-190.2	-49.2	-98.4	-380.3	-42.6
14-RSA-7	-40.9	105.1	60.6	-6.6	189.7	-202.9	-189.7	6.6	-29.0	80.5	188.5	6.6	49.1	-49.1	-134.0	6.6	-78.1	31.4	-7.8	-189.7	-49.1	-98.1	-379.4	-42.5
14-RSA-8	-50.4	126.0	74.8	-7.7	223.7	-239.1	-223.7	7.7	-35.9	96.4	232.0	7.7	57.8	-57.8	-158.1	7.7	-93.7	38.6	0.6	-223.7	-57.8	-115.7	-447.4	-50.1
14-RSA-9	-45.2	114.3	66.9	-7.1	204.3	-218.4	-204.3	7.1	-32.1	87.5	207.7	7.1	52.8	-52.8	-144.4	7.1	-84.9	34.6	-3.7	-204.3	-52.8	-105.7	-408.6	-45.8
14-RSA-10	-56.7	140.4	84.3	-8.7	248.8	-266.1	-248.8	8.7	-40.3	107.4	261.6	8.7	64.4	-64.4	-175.8	8.7	-104.7	43.1	4.1	-248.8	-64.4	-128.7	-497.6	-55.7
14-RSA-11	-42.5	108.6	63.0	-6.8	195.2	-208.7	-195.2	6.8	-30.2	83.1	195.8	6.8	50.5	-50.5	-137.9	6.8	-80.7	32.6	-6.1	-195.2	-50.5	-101.0	-390.4	-43.7
14-RSA-12	-40.6	104.5	60.2	-6.6	188.8	-201.9	-188.8	6.6	-28.8	80.0	187.3	6.6	48.8	-48.8	-133.4	6.6	-77.6	31.2	-8.0	-188.8	-48.8	-97.7	-377.5	-42.3
14-RSA-13	-40.4	104.1	60.0	-6.5	188.2	-201.3	-188.2	6.5	-28.7	79.7	186.5	6.5	48.7	-48.7	-133.0	6.5	-77.4	31.1	-8.2	-188.2	-48.7	-97.4	-376.4	-42.1
14-RSA-14	-40.4	104.0	59.9	-6.5	187.9	-201.0	-187.9	6.5	-28.6	79.6	186.2	6.5	48.6	-48.6	-132.8	6.5	-77.3	31.0	-8.3	-187.9	-48.6	-97.2	-375.9	-42.1
14-RSA-15	-42.3	108.0	62.7	-6.7	194.3	-207.8	-194.3	6.7	-30.0	82.7	194.7	6.7	50.3	-50.3	-137.3	6.7	-80.3	32.5	-6.4	-194.3	-50.3	-100.5	-388.7	-43.5
14-RSA-16	-43.7	111.1	64.7	-6.9	199.1	-212.9	-199.1	6.9	-31.0	85.0	201.0	6.9	51.5	-51.5	-140.7	6.9	-82.5	33.5	-5.0	-199.1	-51.5	-103.0	-398.2	-44.6
14-RSA-17	-45.2	114.3	66.9	-7.1	204.4	-218.5	-204.4	7.1	-32.1	87.5	207.8	7.1	52.9	-52.9	-144.5	7.1	-85.0	34.7	-3.6	-204.4	-52.9	-105.7	-408.8	-45.8
14-RSA-18	-52.6	130.8	78.0	-8.0	231.9	-248.0	-231.9	8.0	-37.4	100.1	241.9	8.0	60.0	-60.0	-163.9	8.0	-97.4	40.1	2.0	-231.9	-60.0	-120.0	-463.9	-52.0
14-RSA-19	-41.1	105.6	61.0	-6.6	190.5	-203.8	-190.5	6.6	-29.2	80.9	189.7	6.6	49.3	-49.3	-134.6	6.6	-78.5	31.6	-7.5	-190.5	-49.3	-98.6	-381.1	-42.7
14-RSA-20	-44.2	112.3	65.5	-6.9	201.0	-214.9	-201.0	6.9	-31.4	85.9	203.5	6.9	52.0	-52.0	-142.1	6.9	-83.4	33.9	-4.5	-201.0	-52.0	-104.0	-402.1	-45.0
14-RSA-21	-44.6	113.2	66.1	-7.0	202.5	-216.5	-202.5	7.0	-31.7	86.6	205.4	7.0	52.4	-52.4	-143.1	7.0	-84.1	34.2	-4.1	-202.5	-52.4	-104.8	-405.0	-45.4
14-RSA-22	-44.8	113.6	66.4	-7.0	203.2	-217.2	-203.2	7.0	-31.9	86.9	206.3	7.0	52.5	-52.6	-143.6	7.0	-84.4	34.4	-3.9	-203.2	-52.5	-105.1	-406.4	-45.5
14-RSA-23	-45.3	114.6	67.1	-7.1	204.9	-219.0	-204.9	7.1	-32.2	87.7	208.4	7.1	53.0	-53.0	-144.8	7.1	-85.2	34.8	-3.5	-204.9	-53.0	-106.0	-409.7	-45.9
14-RSA-24	-46.1	116.3	68.3	-7.2	207.6	-222.0	-207.6	7.2	-32.8	89.0	212.0	7.2	53.7	-53.7	-146.8	7.2	-86.5	35.3	-2.8	-207.6	-53.7	-107.4	-415.3	-46.5
14-RSA-25	-37.2	97.2	55.2	-6.2	177.5	-190.0	-177.5	6.2	-26.3	74.4	171.9	6.2	45.9	-45.9	-125.4	6.2	-72.2	28.5	-11.8	-177.5	-45.9	-91.9	-355.0	-39.7
14-RSA-26	-42.1	107.6	62.4	-6.7	193.6	-207.1	-193.6	6.7	-29.9	82.4	193.8	6.7	50.1	-50.1	-136.8	6.7	-80.0	32.3	-6.6	-193.6	-50.1	-100.2	-387.3	-43.4
14-RSA-28	-39.8	102.8	59.1	-6.5	186.1	-199.0	-186.1	6.5	-28.2	78.7	183.7	6.5	48.1	-48.1	-131.5	6.5	-76.4	30.6	-8.9	-186.1	-48.1	-96.3	-372.1	-41.7
14-RSA-29	-43.8	111.3	64.9	-6.9	199.5	-213.3	-199.5	6.9	-31.1	85.2	201.5	6.9	51.6	-51.6	-141.0	6.9	-82.7	33.6	-4.9	-199.5	-51.6	-103.2	-399.0	-44.7
14-RSA-30	-40.8	104.8	60.4	-6.6	189.2	-202.4	-189.2	6.6	-28.9	80.2	187.9	6.6	48.9	-48.9	-133.7	6.6	-77.9	31.3	-7.9	-189.2	-48.9	-97.9	-378.4	-42.4
14-RSA-31	-47.2	118.8	70.0	-7.3	211.7	-226.3	-211.7	7.3	-33.6	90.9	217.2	7.3	54.8	-54.8	-149.7	7.3	-88.4	36.2	-1.9	-211.7	-54.8	-109.5	-423.5	-47.5
14-RSA-32	-42.6	108.8	63.2	-6.8	195.5	-209.1	-195.5	6.8	-30.3	83.3	196.3	6.8	50.6	-50.6	-138.2	6.8	-80.9	32.7	-6.0	-195.5	-50.6	-101.2	-391.1	-43.8
14-RSA-33	-50.9	126.9	75.4	-7.8	225.3	-240.9	-225.3	7.8	-36.2	97.1	234.0	7.8	58.3	-58.3	-159.3	7.8	-94.5	38.9	0.9	-225.3	-58.3	-116.5	-450.6	-50.5
14-RSA-34	-42.0	107.6	62.3	-6.7	193.6	-207.0	-193.6	6.7	-29.9	82.4	193.7	6.7	50.1	-50.1	-136.8	6.7	-79.9	32.3	-6.6	-193.6	-50.1	-100.1	-387.2	-43.4
14-RSA-37	-44.0	111.9	65.3	-6.9	200.4	-214.3	-200.4	6.9	-31.3	85.6	202.7	6.9	51.8	-51.8	-141.7	6.9	-83.1	33.8	-4.7	-200.4	-51.8	-103.7	-400.9	-44.9

Appendix C *continued*

#	logK																								
	2400-1	2400-2	2400-5	2400-21	2400-22	2400-23	2500-24	2400-25	2500-1	2500-2	2500-5	2500-21	2500-22	2500-23	2500-24	2500-25	2600-1	2600-2	2600-5	2600-21	2600-22	2600-23	2600-24	2600-25	
14-RSA-1	20,7	140,4	419,2	218,5	52,9	105,7	119,8	59,9	-5,4	194,0	538,9	204,4	144,5	408,7	-119,8	59,9	-13,1	26,8	59,8	-7,1	-7,1	45,8	-59,9	-59,9	
14-RSA-2	24,3	173,5	524,3	268,7	65,0	130,0	147,5	73,8	-8,7	239,9	677,2	251,2	177,5	502,4	-147,5	73,8	-16,5	33,2	76,4	-8,8	-8,8	56,2	-73,8	-73,8	
14-RSA-3	21,0	143,9	430,6	223,7	54,1	108,3	122,7	61,4	-5,9	199,0	554,1	209,3	148,0	418,6	-122,7	61,4	-13,4	27,5	61,7	-7,2	-7,2	46,9	-61,4	-61,4	
14-RSA-4	20,0	128,5	381,5	201,4	48,7	97,4	110,5	55,3	-3,5	177,3	488,5	188,3	133,0	376,6	-110,5	55,3	-11,8	24,4	53,5	-6,5	-6,5	42,2	-55,3	-55,3	
14-RSA-5	24,4	174,8	528,4	270,8	65,5	131,0	148,6	74,3	-8,8	241,7	682,5	253,1	178,8	506,2	-148,6	74,3	-16,6	33,5	77,0	-8,8	-8,8	56,6	-74,3	-74,3	
14-RSA-6	20,1	129,9	385,9	203,4	49,2	98,4	111,6	55,8	-3,7	179,3	494,4	190,2	134,4	380,3	-111,6	55,8	-11,9	24,7	54,2	-6,6	-6,6	42,6	-55,8	-55,8	
14-RSA-7	20,0	129,5	384,8	202,9	49,1	98,1	111,3	55,7	-3,7	178,8	492,9	189,7	134,0	379,4	-111,3	55,7	-11,9	24,6	54,1	-6,6	-6,6	42,5	-55,7	-55,7	
14-RSA-8	22,0	154,3	463,4	239,1	57,8	115,7	131,1	65,6	-7,1	213,4	597,5	223,7	158,1	447,4	-131,1	65,6	-14,5	29,6	67,0	-7,7	-7,7	50,1	-65,6	-65,6	
14-RSA-9	20,7	140,3	419,1	218,4	52,8	105,7	119,8	59,9	-5,4	193,9	538,7	204,3	144,4	408,6	-119,8	59,9	-13,1	26,8	59,8	-7,1	-7,1	45,8	-59,9	-59,9	
14-RSA-10	24,0	171,8	519,1	266,1	64,4	128,7	146,0	73,0	-8,6	237,7	670,4	248,8	175,8	497,6	-146,0	73,0	-16,3	32,9	75,6	-8,7	-8,7	55,7	-73,0	-73,0	
14-RSA-11	20,3	133,6	397,8	208,7	50,5	101,0	114,5	57,2	-4,4	184,5	510,3	195,2	137,9	390,4	-114,5	57,2	-12,3	25,5	56,3	-6,8	-6,8	43,7	-57,2	-57,2	
14-RSA-12	20,0	128,8	382,6	201,9	48,8	97,7	110,8	55,4	-3,6	177,8	489,9	188,8	133,4	377,5	-110,8	55,4	-11,8	24,5	53,7	-6,6	-6,6	42,3	-55,4	-55,4	
14-RSA-13	20,0	128,4	381,3	201,3	48,7	97,4	110,5	55,2	-3,5	177,2	488,2	188,2	133,0	376,4	-110,5	55,2	-11,7	24,4	53,4	-6,5	-6,5	42,1	-55,2	-55,2	
14-RSA-14	20,0	128,2	380,6	201,0	48,6	97,2	110,3	55,2	-3,5	176,9	487,3	187,9	132,8	375,9	-110,3	55,2	-11,7	24,4	53,3	-6,5	-6,5	42,1	-55,2	-55,2	
14-RSA-15	20,2	133,0	395,8	207,8	50,3	100,5	114,0	57,0	-4,3	183,6	507,6	194,3	137,3	388,7	-114,0	57,0	-12,3	25,3	55,9	-6,7	-6,7	43,5	-57,0	-57,0	
14-RSA-16	20,5	136,5	407,0	212,9	51,5	103,0	116,8	58,4	-4,8	188,6	522,6	199,1	140,7	398,2	-116,8	58,4	-12,6	26,0	57,8	-6,9	-6,9	44,6	-58,4	-58,4	
14-RSA-17	20,7	140,4	419,3	218,5	52,9	105,7	119,9	59,9	-5,4	194,0	539,1	204,4	144,5	408,8	-119,9	59,9	-13,1	26,8	59,9	-7,1	-7,1	45,8	-59,9	-59,9	
14-RSA-18	22,6	160,1	481,9	248,0	60,0	120,0	136,0	68,0	-7,7	221,5	621,8	231,9	163,9	463,9	-136,0	68,0	-15,1	30,7	70,0	-8,0	-8,0	52,0	-68,0	-68,0	
14-RSA-19	20,1	130,2	386,8	203,8	49,3	98,6	111,8	55,9	-3,8	179,7	495,6	190,5	134,6	381,1	-111,8	55,9	-11,9	24,8	54,4	-6,6	-6,6	42,7	-55,9	-55,9	
14-RSA-20	20,6	137,9	411,5	214,9	52,0	104,0	117,9	58,9	-5,0	190,6	528,6	201,0	142,1	402,1	-117,9	58,9	-12,8	26,3	58,6	-6,9	-6,9	45,0	-58,9	-58,9	
14-RSA-21	20,6	139,0	414,9	216,5	52,4	104,8	118,7	59,4	-5,2	192,1	533,2	202,5	143,1	405,0	-118,7	59,4	-12,9	26,5	59,1	-7,0	-7,0	45,4	-59,4	-59,4	
14-RSA-22	20,7	139,5	416,5	217,2	52,6	105,1	119,1	59,6	-5,2	192,8	535,2	203,2	143,6	406,4	-119,1	59,6	-13,0	26,6	59,4	-7,0	-7,0	45,5	-59,6	-59,6	
14-RSA-23	20,8	140,7	420,4	219,0	53,0	106,0	120,1	60,1	-5,4	194,5	540,5	204,9	144,8	409,7	-120,1	60,1	-13,1	26,9	60,0	-7,1	-7,1	45,9	-60,1	-60,1	
14-RSA-24	20,9	142,7	426,8	222,0	53,7	107,4	121,7	60,9	-5,7	197,3	549,0	207,6	146,8	415,3	-121,7	60,9	-13,3	27,3	61,1	-7,2	-7,2	46,5	-60,9	-60,9	
14-RSA-25	19,6	120,4	355,6	190,0	45,9	91,9	104,3	52,2	-2,1	165,9	453,6	177,5	125,4	355,0	-104,3	52,2	-10,8	22,7	49,0	-6,2	-6,2	39,7	-52,2	-52,2	
14-RSA-26	20,2	132,5	394,1	207,1	50,1	100,2	113,6	56,8	-4,2	182,9	505,4	193,6	136,8	387,3	-113,6	56,8	-12,2	25,2	55,6	-6,7	-6,7	43,4	-56,8	-56,8	
14-RSA-28	19,9	126,8	376,2	199,0	48,1	96,3	109,2	54,6	-3,2	175,0	481,4	186,1	131,5	372,1	-109,2	54,6	-11,6	24,1	52,6	-6,5	-6,5	41,7	-54,6	-54,6	
14-RSA-29	20,5	136,8	407,8	213,3	51,6	103,2	117,0	58,5	-4,8	189,0	523,7	199,5	141,0	399,0	-117,0	58,5	-12,7	26,1	58,0	-6,9	-6,9	44,7	-58,5	-58,5	
14-RSA-30	20,0	129,2	383,7	202,4	48,9	97,9	111,1	55,5	-3,6	178,3	491,4	189,2	133,7	378,4	-111,1	55,5	-11,8	24,6	53,9	-6,6	-6,6	42,4	-55,5	-55,5	
14-RSA-31	21,2	145,7	436,2	226,3	54,8	109,5	124,1	62,1	-6,1	201,5	561,5	211,7	149,7	423,5	-124,1	62,1	-13,6	27,9	62,7	-7,3	-7,3	47,5	-62,1	-62,1	
14-RSA-32	20,3	133,9	398,6	209,1	50,6	101,2	114,7	57,3	-4,4	184,9	511,4	195,5	138,2	391,1	-114,7	57,3	-12,3	25,5	56,4	-6,8	-6,8	43,8	-57,3	-57,3	
14-RSA-33	22,1	155,4	467,1	240,9	58,3	116,5	132,1	66,0	-7,2	215,0	602,3	225,3	159,3	450,6	-132,1	66,0	-14,7	29,8	67,6	-7,8	-7,8	50,5	-66,0	-66,0	
14-RSA-34	20,2	132,4	394,0	207,0	50,1	100,1	113,6	56,8	-4,2	182,9	505,2	193,6	136,8	387,2	-113,6	56,8	-12,2	25,2	55,6	-6,7	-6,7	43,4	-56,8	-56,8	
14-RSA-37	20,5	137,5	410,1	214,3	51,8	103,7	117,5	58,8	-4,9	190,0	526,7	200,4	141,7	400,9	-117,5	58,8	-12,7	26,2	58,3	-6,9	-6,9	44,9	-58,8	-58,8	

Appendix D

Calculated reaction affinity (kcal/mol e⁻) for the reactions of interest

#	t°C	pHT	kcal/mole ⁻																					
			100-1	100-20	100-21	100-22	100-23	100-24	100-25	200-1	200-20	200-21	200-22	200-23	200-24	200-25	500-1	500-2	500-20	500-21	500-22	500-23	500-24	500-25
14-RSA-1	69	7,27	-23,9	-9,3		-21,3		-2,0		23,9	14,6	15,9	2,6		21,9		21,9	-2,0	23,4		0,6		19,3	
14-RSA-2	4	9,26																						
14-RSA-3	60	8,74	-22,8		-9,9	-21,4	1,6			29,8		12,9	1,4	24,4			21,7	-1,1		11,9	0,4	23,4		
14-RSA-4	100	8,34																	24,0	11,4			14,9	
14-RSA-5	2	9,32																						
14-RSA-6	96	8,26		-10,4	-11,2	-22,4	0,1	-3,2	-8,1								22,6		23,7	11,5	0,3	22,7	18,7	14,5
14-RSA-7	97	8,13		-9,6	-10,4	-21,8	1,0	-2,3	-7,3								21,8		23,6	11,5	0,1	22,9	18,9	14,6
14-RSA-8	38	7,27	-23,9	-9,5		-21,8		-2,2		31,7	14,4	15,3	2,1		21,7									
14-RSA-9	69	7,36																						
14-RSA-10	7	7,70																						
14-RSA-11	86	7,41		-9,8	-10,5	-22,0	1,1	-2,4	-7,6								22,0		23,2	11,5	0,0	23,1	19,0	14,4
14-RSA-12	99	8,16	-22,2	-9,7	-10,5	-21,8	0,8	-2,4	-7,1	28,3	12,6	11,7	0,4	23,0	19,9	15,1	21,9	-0,3	23,6	11,4	0,1	22,7	18,8	14,8
14-RSA-13	100	8,21																	23,6	11,4				14,6
14-RSA-14	101	8,15		-9,8	-10,6	-21,8	0,6	-2,5	-7,3								22,0		23,7	11,4	0,2	22,6	18,8	14,7
14-RSA-15	87	7,93	-23,1			-21,8				29,6		14,5	1,3				22,0	-1,1			0,2			
14-RSA-16	78	8,82				-22,0											22,0				0,0			
14-RSA-17	68	8,95	-23,9	-10,1		-22,1		-2,8		31,0	13,8	14,8	1,8		21,0		22,4	-1,5	24,3		0,3		18,8	
14-RSA-18	27	9,72				-22,7											23,1				0,3			
14-RSA-19	95	8,70		-9,9	-10,7	-22,0	0,5	-2,6	-7,3								22,0		24,0	11,3	0,0	22,6	18,7	14,7
14-RSA-20	75	8,49		-9,9		-22,2		-2,6									22,2		23,9		0,0		18,9	
14-RSA-21	72	8,85	-22,6	-9,9	-10,6	-21,5	0,4	-2,9	-7,9	29,3	12,7	12,0	1,1	22,9	19,6	14,7	22,4	-0,2	24,3	11,9	1,0	22,8	18,8	14,5
14-RSA-22	71	9,23		-10,2	-10,7	-21,7	0,3	-3,3	-8,7								22,8		24,8	12,1	1,1	23,1	18,7	14,0
14-RSA-23	68	9,21		-10,1	-10,8	-22,0	0,4	-2,9	-7,8								22,4		24,5	11,6	0,4	22,8	18,8	14,6
14-RSA-24	63	9,69	-24,0	-10,0	-10,9	-22,0	0,1	-2,8	-7,2	31,2	14,0	13,0	2,0	24,1	21,2	16,8								17,0
14-RSA-25	125	8,22	-22,0	-9,5	-10,3	-21,3	0,6	-2,4	-6,9	27,7	12,5	11,7	0,7	22,6	19,6	15,1	21,5	-0,5	23,8	11,2	0,3	22,1	18,4	14,6
14-RSA-26	89	8,92	-23,5		-10,6	-21,5	0,3			30,1		12,9	2,0	23,8			22,0	-1,5		11,4	0,5	22,3		
14-RSA-28	105	7,80			-10,1	-21,5	1,4										21,3			11,2	-0,2	22,6		
14-RSA-29	77	8,86	-22,7	-9,5		-21,4		-2,4		29,3	13,1	14,2	1,3		20,3		21,8	-0,9	24,3		0,4		18,7	
14-RSA-30	98	3,01		-8,0		-20,5		-0,5																
14-RSA-31	56	3,19		-8,2		-20,3		-0,9																
14-RSA-32	85	3,26		-8,0		-20,1		-0,8																
14-RSA-33	36	4,35																						
14-RSA-34	89	2,94																						
14-RSA-37	76	2,48																					14,7	

Appendix D *continued*

#	kcal/mole ⁻																								
	2100-1	2100-2	2100-5	2100-21	2100-22	2100-23	2100-24	2100-25	2200-1	2200-3	2200-5	2200-21	2200-22	2200-23	2200-24	2200-25	2300-1	2300-2	2300-5	2300-21	2300-22	2300-23	2300-24	2300-25	
14-RSA-1	9,3	-14,6	-12,6		-12,1		7,2											21,3	-2,6	-0,6	12,1				19,3
14-RSA-2																									
14-RSA-3																									
14-RSA-4																									
14-RSA-5																									
14-RSA-6	10,4		-12,3	-0,8	-12,0	10,5	7,2	2,3	11,2		-11,5	0,8	-11,2	11,2	7,9	3,0	22,4		-0,3	12,0	11,2	22,4	19,2	14,3	
14-RSA-7	9,6		-12,2	-0,8	-12,2	10,6	7,3	2,3	10,4		-11,5	0,8	-11,4	11,4	8,1	3,1	21,8		-0,1	12,2	11,4	22,8	19,5	14,5	
14-RSA-8	9,5	-14,4			-12,3		7,4											21,8	-2,1		12,3				19,6
14-RSA-9																									
14-RSA-10																									
14-RSA-11	9,8		-12,2	-0,7	-12,3	10,8	7,4	2,2	10,5		-11,5	0,7	-11,5	11,5	8,1	2,9	22,0		0,0	12,3	11,5	23,1	19,6	14,5	
14-RSA-12	9,7	-12,6	-12,2	-0,9	-12,2	10,4	7,3	2,6	10,5	-11,7	-11,4	0,9	-11,3	11,3	8,2	3,4	21,8	-0,4	-0,1	12,2	11,3	22,6	19,5	14,7	
14-RSA-13																									
14-RSA-14	9,8		-12,2	-0,8	-12,1	10,4	7,2	2,5	10,6		-11,4	0,8	-11,2	11,2	8,1	3,3	21,8		-0,2	12,1	11,2	22,5	19,3	14,5	
14-RSA-15																		21,8	-1,3	-0,2					
14-RSA-16																		22,0	0,0						
14-RSA-17	10,1	-13,8	-12,3		-12,0		7,2											22,1	-1,8	-0,3	12,0				19,3
14-RSA-18																		22,7	-0,3						
14-RSA-19	9,9		-12,2	-0,8	-12,1	10,4	7,3	2,5	10,7		-11,3	0,8	-11,3	11,3	8,1	3,4	22,0		0,0	12,1	11,3	22,5	19,4	14,7	
14-RSA-20	9,9		-12,3		-12,3		7,4											22,2	0,0	12,3				19,6	
14-RSA-21	9,9	-12,7	-12,5	-0,7	-11,6	10,2	6,9	2,0	10,6	-12,0	-11,9	0,7	-10,9	10,9	7,6	2,6	21,5	-1,1	-1,0	11,6	10,9	21,8	18,5	13,6	
14-RSA-22	10,2		-12,6	-0,5	-11,5	10,5	6,9	1,5	10,7		-12,1	0,5	-11,0	11,0	7,4	1,9	21,7		-1,1	11,5	11,0	22,0	18,3	12,9	
14-RSA-23	10,1		-12,3	-0,8	-12,0	10,5	7,2	2,3	10,8		-11,6	0,8	-11,2	11,2	7,9	3,0	22,0		-0,4	12,0	11,2	22,4	19,1	14,2	
14-RSA-24	10,0	-14,0		-0,9	-12,0	10,1	7,2	2,8	10,9	-13,0		0,9	-11,1	11,1	8,1	3,8	22,0	-2,0		12,0	11,1	22,1	19,2	14,8	
14-RSA-25	9,5	-12,5	-12,1	-0,9	-11,8	10,1	7,1	2,6	10,3	-11,7	-11,2	0,9	-10,9	10,9	7,9	3,4	21,3	-0,7	-0,3	11,8	10,9	21,9	18,9	14,4	
14-RSA-26									10,6	-12,9	-11,4		-10,9	10,9			21,5	-2,0	-0,5			10,9	21,9		
14-RSA-28									10,1		-11,2		-11,4	11,4			21,5	0,2		11,4	22,8				
14-RSA-29	9,5	-13,1	-12,3		-11,9		7,1										21,4	-1,3	-0,4	11,9				19,0	
14-RSA-30	8,0				-12,5		7,5										20,5			12,5				20,0	
14-RSA-31	8,2				-12,1		7,3										20,3			12,1				19,4	
14-RSA-32	8,0				-12,1		7,2										20,1			12,1				19,3	
14-RSA-33																									
14-RSA-34					-0,5			1,4				0,5				1,8									
14-RSA-37																									

Appendix D *continued*

Appendix E

Further information on sampling locations

#	Date	Location	Type	Lat	Long	t°C	pH _T
14-RSA-1	13.5.14	Hveragerdi	Hot spring	64.00197	-21.18139	69	7.27
14-RSA-2	13.5.14	Ingólfssjall	Cold water	63.96374	-20.99992	4	9.26
14-RSA-3	13.5.14	Laugarbakkar	Well	63.96598	-20.97430	60	8.74
14-RSA-4	13.5.14	Laugarvatn	Hot spring	64.21543	-20.73196	100	8.34
14-RSA-5	13.5.14	Vellankatla	Cold water	64.24437	-21.08057	2	9.32
14-RSA-6	14.5.14	Sísjódandi	Hot spring	64.31032	-20.30670	96	8.26
14-RSA-7	14.5.14	Ótherrhíðar	Hot spring	64.31112	-20.30573	97	8.13
14-RSA-8	14.5.14	Haukadalur	Hot spring	64.32740	-20.28326	38	7.27
14-RSA-9	14.5.14	Nedridalur	Well	64.30118	-20.33214	69	7.36
14-RSA-10	14.5.14	Lyngdalsheidi	Cold water	64.21302	-20.77733	7	7.70
14-RSA-11	22.5.14	Marteinslaug	Hot spring	64.33178	-20.28713	86	7.41
14-RSA-12	22.5.14	Vadmálahver	Hot spring	64.13695	-20.30955	99	8.16
14-RSA-13	22.5.14	Flúdir	Well	64.13676	-20.31161	100	8.21
14-RSA-14	22.5.14	Flúdir	Well	64.12922	-20.32370	101	8.15
14-RSA-15	22.5.14	Sólheimar	Well	64.06925	-20.64405	87	7.93
14-RSA-16	16.7.14	Oddgeirshíðar	Well	63.98204	-20.85921	78	8.82
14-RSA-17	16.7.14	Reykholll	Well	64.04426	-20.44828	68	8.95
14-RSA-18	16.7.14	Sóleyjarbakki	Well	64.06644	-20.39582	27	9.72
14-RSA-19	16.7.14	Bergsstadir	Well	64.20732	-20.35056	95	8.70
14-RSA-20	16.7.14	Spóastadir	Well	64.14730	-20.55360	75	8.49
14-RSA-21	5.8.14	Húnavellir (well 21)	Well	65.54138	-20.21392	72	8.85
14-RSA-22	5.8.14	Siglufjördur (well 11)	Well	66.11719	-18.87759	71	9.23
14-RSA-23	11.8.14	Borgarmýrar	Well	65.73315	-19.61507	68	9.21
14-RSA-24	8.8.14	Laugarin Reykjadalur	Well	65.72263	-17.35460	63	9.69
14-RSA-25	8.8.14	Hveravellir	Well	65.88846	-17.30632	125	8.22
14-RSA-26	8.8.14	Reykir in Fnjóskadalur	Well	65.57628	-17.76370	89	8.92
14-RSA-28	3.9.14	Bakki II	Well	63.94480	-21.27018	105	7.80
14-RSA-29	3.9.14	Mosfellsdalur	Well	64.15766	-21.65130	77	8.86
14-RSA-30	8.9.14	Hveragerdi	Hot spring	64.00655	-21.18138	98	3.01
14-RSA-31	8.9.14	Hveragerdi	Hot spring	64.00655	-21.18138	56	3.19
14-RSA-32	8.9.14	Hveragerdi	Hot spring	64.00655	-21.18138	85	3.26
14-RSA-33	8.9.14	Hveragerdi	Hot spring	64.00655	-21.18138	36	4.35
14-RSA-34	8.9.14	Hveragerdi	Hot spring	64.00655	-21.18138	89	2.94
14-RSA-37	8.9.14	Hveragerdi	Hot spring	64.00655	-21.18138	76	2.48